

VOTCA-XTP

EXCITON TRANSPORT SIMULATIONS

USER MANUAL



compiled from: (0c0a762)

September 15, 2016

www.votca.org

Disclaimer

This manual is not complete. The best way to start using the software is to look at provided tutorials. The reference section is generated automatically from the source code, so please make sure that your software and manual versions match.

Citations

Development of this software depends on academic research grants. If you are using the package, please cite the following papers

[1] Microscopic simulations of charge transport in disordered organic semiconductors, Victor Rühle, Alexander Lukyanov, Falk May, Manuel Schrader, Thorsten Vehoff, James Kirkpatrick, Björn Baumeier and Denis Andrienko
J. Chem. Theor. Comp. **7**, 3335, 2011

[2] Versatile Object-oriented Toolkit for Coarse-graining Applications
Victor Rühle, Christoph Junghans, Alexander Lukyanov, Kurt Kremer and Denis Andrienko
J. Chem. Theor. Comp. **5**, 3211, 2009

Development

The core development is currently taking place at the Max Planck Institute for Polymer Research, Mainz, Germany and TU/e Eindhoven.

Copyright

VOTCA-XTP is free software. The entire package is available under the Apache License. For details, check the LICENSE file in the source code. The VOTCA-XTP source code is available on our homepage, www.votca.org.

Contents

1	Introduction	3
2	Theoretical background	5
2.1	Workflow	5
2.2	Material morphology	5
2.3	Conjugated segments and rigid fragments	6
2.4	Neighbor list	7
2.5	Reorganization energy	8
2.5.1	Intramolecular reorganization energy	8
2.5.2	Outersphere reorganization energy	8
2.6	Site energies	9
2.6.1	Externally applied electric field	10
2.6.2	Internal energy	10
2.6.3	Electrostatic interaction energy	10
2.6.4	Induction energy - the Thole model	11
2.7	Transfer integrals	13
2.7.1	Projection of monomer orbitals on dimer orbitals (DIPRO)	13
2.7.2	DFT-based transfer integrals using DIPRO	15
2.7.3	ZINDO-based transfer integrals using MOO	17
2.8	Charge transfer rate	17
2.8.1	Classical charge transfer rate	17
2.8.2	Semi-classical bimolecular rate	18
2.8.3	Semi-classical rate	18
2.9	Master equation	19
2.9.1	Extrapolation to nondispersive mobilities	19
2.10	Macroscopic observables	19
2.10.1	Charge density	20
2.10.2	Current	20
2.10.3	Mobility and diffusion constant	21
2.10.4	Spatial correlations of energetic disorder	21
3	Input and output files	23
3.1	Atomistic topology	23
3.2	Mapping file	25
3.3	Molecular orbitals	26
3.4	Monomer calculations for DFT transfer integrals	27
3.5	Pair calculations for DFT transfer integrals	29
3.6	DFT transfer integrals	30
3.7	State file	31

4	Reference	33
4.1	Programs	33
4.1.1	xtp_testsuite	33
4.1.2	xtp_update	33
4.1.3	xtp_update_exciton	33
4.1.4	xtp_basisset	33
4.1.5	xtp_map	34
4.1.6	xtp_run	34
4.1.7	xtp_tools	34
4.1.8	xtp_parallel	34
4.1.9	xtp_dump	35
4.1.10	xtp_overlap	35
4.1.11	xtp_kmc_run	35
4.2	Calculators	35
4.2.1	coupling	36
4.2.2	excitoncoupling	36
4.2.3	gencube	37
4.2.4	log2mps	37
4.2.5	molpol	37
4.2.6	orb2isogwa	38
4.2.7	partialcharges	38
4.2.8	pdb2map	38
4.2.9	pdb2top	38
4.2.10	ptopreader	38
4.2.11	qmanalyze	39
4.2.12	eanalyze	39
4.2.13	eimport	39
4.2.14	einternal	39
4.2.15	emultipole	39
4.2.16	eoutersphere	40
4.2.17	ianalyze	40
4.2.18	iimport	41
4.2.19	izindo	41
4.2.20	jobwriter	41
4.2.21	pairdump	41
4.2.22	panalyze	41
4.2.23	profile	42
4.2.24	rates	42
4.2.25	sandbox	42
4.2.26	stateserver	43
4.2.27	tdump	43
4.2.28	vaverage	43
4.2.29	zmultipole	43
4.2.30	edft	44
4.2.31	egwbse	44
4.2.32	idft	44
4.2.33	igwbse	45
4.2.34	qmmm	45
4.2.35	xqmultipole	46
4.2.36	energy2xml	46
4.2.37	integrals2xml	47
4.2.38	occupations2xml	47
4.2.39	pairs2xml	47
4.2.40	rates2xml	47

CONTENTS

v

4.2.41	segments2xml	47
4.2.42	trajectory2pdb	47
4.3	Common options	48
Bibliography		49

Index

- charge transfer rate, 17
 - bimolecular, 18
 - classical, 17
 - semiclassical, 18
- conjugated segment, 6
- current, 20
 - local, 20
- diabatic states, 13
- distributed multipoles, 10
- electronic coupling, 13
 - DFT, 15
 - ZINDO, 17
- hopping site, 6
- kinetic Monte Carlo, 19
- mobility, 21
- neighbor list, 7
- Pekar factor, 9
- reorganization energy, 8
 - intramolecular, 8
 - outersphere, 8
- rigid fragment, 7
- site energy, 9
 - distributed multipoles, 10
 - external field, 10
 - internal, 10
 - polarization, 11
 - spatial correlation, 21
- Thole model, 11
- transfer integral, *see* electronic coupling

Chapter 1

Introduction

sec:introduction

Charge carrier dynamics in an organic semiconductor can often be described in terms of charge hopping between localized states. The hopping rates depend on **electronic coupling elements**, **reorganization energies**, and **site energies**, which vary as a function of position and orientation of the molecules. The purpose of the VOTCA-XTP package [1] is to simplify the workflow for charge transport simulations, provide a uniform error-control for the methods, flexible platform for their development, and eventually allow *in silico* prescreening of organic semiconductors for specific applications.

The toolkit is implemented using modular concepts introduced earlier in the Versatile Object-oriented Toolkit for Coarse-graining Applications (VOTCA) [2]. It contains different **programs**, which execute specific tasks implemented in **calculators** representing an individual step in the workflow. Figure 1.1 summarizes a typical chain of commands to perform a charge transport simulation: First, the VOTCA code structures are adapted to reading atomistic trajectories, mapping them onto **conjugated segments and rigid fragments**, and substituting (if needed) rigid fragments with the optimized copies (**xtp_map**). The programs **xtp_run** and **xtp_parallel** (for heavy-duty tasks) are then used to calculate all bimolecular charge hopping rates (via precalculation of all required ingredients). **Site energies (or energetic disorder)** can be determined as a combination of internal (ionization potentials/electron affinities of single molecules) as well as electrostatic and polarization contributions within the molecular environment. The calculation of **electronic coupling elements** between conjugated segments from the corresponding molecular orbitals can be performed using a **dimer-projection** technique based on **density-functional** theory (DFT). This requires explicit calculations using quantum-chemistry software for which we provide interfaces to Gaussian, Turbomole, and NWChem. Alternatively, the **molecular orbital overlap** module calculates electronic coupling elements relying on the semi-empirical INDO Hamiltonian and molecular orbitals in the format provided by the Gaussian package.

The **kinetic Monte Carlo** module reads in the **neighbor list**, **site coordinates**, and **hopping rates** and performs charge dynamics simulations using either periodic boundary conditions or charge sources and sinks.

The toolkit is written as a combination of modular C++ code and scripts. The data transfer between programs is implemented via a **state file** (sql database), which is also used to restart simulations. Analysis functions and most of the calculation routines are encapsulated by using the observer pattern [3] which allows the implementation of new functions as individual modules.

In the following chapter 2, we summarize the **theoretical background** of the workflow of charge transport simulations and in particular its individual steps. Chapter 3 describes the structure and content of input and output files, while a full reference of **programs** and **calculators** is available in chapter 4. For a hands-on tutorial, the reader is referred to the **VOTCA-XTP** project page at <http://code.google.com/p/votca-xtp/>.

Figure 1.1: A practical workflow of charge transport simulations using VOTCA-XTP. The **theoretical background** of the individual steps is given in chapter 2. Chapter 3 describes the content of input and output files, while a full reference of **programs** and **calculators** is available in chapter 4.

fig:summary

Chapter 2

Theoretical background

2.1 Workflow

A typical workflow of charge transport simulations is depicted in figure 2.1. The first step is the simulation of an **atomistic morphology**, which is then partitioned on **hopping sites**. The coordinates of the hopping sites are used to construct a list of pairs of molecules, or **neighbor list**.



Figure 2.1: Workflow for microscopic simulations of charge transport.

For each pair an **electronic coupling element**, a **reorganization energy**, a **driving force**, and eventually the **hopping rate** are evaluated. The neighbor list and hopping rates define a directed graph. The corresponding master equation is solved using the **kinetic Monte Carlo** method, which allows to explicitly monitor the charge dynamics in the system as well as to calculate time or ensemble averages of occupation probabilities, charge fluxes, correlation functions, and field-dependent mobilities.

2.2 Material morphology

There is no generic recipe on how to predict a large-scale atomistically-resolved morphology of an organic semiconductor. The required methods are system-specific: for ultra-pure crystals, for



Figure 2.2: The concept of conjugated segments and rigid fragments. Dashed lines indicate conjugated segments while colors denote rigid fragments. (a) Hexabenzocoronene: the π -conjugated system is both a rigid fragment and a conjugated segment. (b) Alq_3 : the Al atom and each ligand are rigid fragments while the whole molecule is a conjugated segment. (c) Polythiophene: each repeat unit is a rigid fragment. A conjugated segment consists of one or more rigid fragments. One molecule can have several conjugated segments.

fig:segment

example, density-functional methods can be used provided the crystal structure is known from experiment. For partially disordered organic semiconductors, however, system sizes much larger than a unit cell are required. Classical molecular dynamics or Monte Carlo techniques are then the methods of choice.

In molecular dynamics, atoms are represented by point masses which interact via empirical potentials prescribed by a force-field. Force-fields are parametrized for a limited set of compounds and their refinement is often required for new molecules. In particular, special attention shall be paid to torsion potentials between successive repeat units of conjugated polymers or between functional groups and the π -conjugated system. First-principles methods can be used to characterize the missing terms of the potential energy function.

Self-assembling materials, such as soluble oligomers, discotic liquid crystals, block copolymers, partially crystalline polymers, etc., are the most complicated to study. The morphology of such systems often has several characteristic length scales and can be kinetically arrested in a thermodynamically non-equilibrium state. For such systems, the time- and length-scales of atomistic simulations might be insufficient to equilibrate or sample desired morphologies. In this case, systematic coarse-graining can be used to enhance sampling [2]. Note that the coarse-grained representation must reflect the structure of the atomistic system and allow for back-mapping to the atomistic resolution.

Here we assume that the morphology is already known, that is we know how the topology and the coordinates of all atoms in the systems at a given time. VOTCA-XTP can read standard GROMACS topology files. Custom definitions of **atomistic topology** via XML files are also possible. Since the description of the atomistic topology is the first step in the charge transport simulations, it is important to follow simple conventions on how the system is partitioned on molecules, residues, and how atoms are named in the topology. Required input files are described in section **atomistic topology**.

2.3 Conjugated segments and rigid fragments

sec:segments

With the morphology at hand, the next step is partitioning the system on hopping sites, or conjugated segments, and calculating charge transfer rates between them. Physically intuitive arguments can be used for the partitioning, which reflects the localization of the wave function of a charge. For most organic semiconductors, the molecular architecture includes relatively rigid, planar π -conjugated systems, which we will refer to as rigid fragments. A conjugated segment can contain one or more of such rigid fragments, which are linked by bonded degrees of freedom.

The dynamics of these degrees of freedom evolves on timescales much slower than the frequency of the internal promoting mode. In some cases, e.g. glasses, it can be ‘frozen’ due to non-bonded interactions with the surrounding molecules.

To illustrate the concept of conjugated segments and rigid fragments, three representative molecular architectures are shown in figure 2.2. The first one is a typical discotic liquid crystal, hexabenzocoronene. It consists of a conjugated core to which side chains are attached to aid self-assembly and solution processing. In this case the orbitals localized on side chains do not participate in charge transport and the conjugated π -system is both, a rigid fragment and a conjugated segment. In Alq_3 , a metal-coordinated compound, a charge carrier is delocalized over all three ligands. Hence, the whole molecule is one conjugated segment. Individual ligands are relatively rigid, while energies of the order of $k_B T$ are sufficient to reorient them with respect to each other. Thus the Al atom and the three ligands are rigid fragments. In the case of a conjugated polymer, one molecule can consist of several conjugated segments, while each backbone repeat unit is a rigid fragment. Since the conjugation along the backbone can be broken due to large out-of-plane twists between two repeat units, an empirical criterion, based on the dihedral angle, can be used to partition the backbone on conjugated segments [4]. However, such intuitive partitioning is, to some extent, arbitrary and shall be validated by other methods [5–7].

After partitioning, an additional step is often required to remove bond length fluctuations introduced by molecular dynamics simulations, since they are already integrated out in the derivation of the rate expression. This is achieved by substituting respective molecular fragments with rigid, planar π -systems optimized using first-principles methods. Centers of mass and gyration tensors are used to align rigid fragments, though a custom definition of local axes is also possible. Such a procedure also minimizes discrepancies between the force-field and first-principles-based ground state geometries of conjugated segments, which might be important for calculations of electronic couplings, reorganization energies, and intramolecular driving forces.

To partition the system on hopping sites and substitute rigid fragments with the corresponding ground-state geometries `xtp_map` program is used: `xtp_map -t topol.tpr -c traj.xtc -s map.xml -f state.sql` It reads in the GROMACS topology (`topol.tpr`) and trajectory (`traj.xtc`) files, definitions of conjugated segments and rigid fragments (`map.xml`) and outputs coordinates of conjugated segments (hopping sites) and rigid fragments (as provided in the MD trajectory and after rigidification) to the state file (`state.sql`). In order to do this, a mapping file `map.xml` has to be provided, which specifies the corresponding atoms in the different representations. After this step, all information (frame number, dimensions of the simulation box, etc) are stored in the `state` file and only this file is used for further calculations.

VOTCA-XTP requires a wrapped trajectory for mapping the segments and fragments, so all molecules should be whole in the frame.

In order to visually check the mapping one can use either the `tdump` calculator or the program `xtp_dump` with the calculator `trajectory2pdb`.

```
xtp_dump -f state.sql -e trajectory2pdb
```

It reads in the state file created by `xtp_map` and outputs two trajectory files corresponding to the original and rigidified atom coordinates. To check the mapping, it is useful to superimpose the three outputs (original atomistic, atomistic stored in the state file, and rigidified according to ground state geometries), e.g., with VMD.

```
xtp_run -f state.sql -o options.xml -e tdump
```

It also reads in the state file but appends the coordinates to a `pdb` file. So make sure to delete old `QM.pdb` and `MD.pdb` if you want to create a new imagef

2.4 Neighbor list

A list of neighboring conjugated segments, or neighbor list, contains all pairs of conjugated segments for which *coupling elements*, *reorganization energies*, *site energy differences*, and *rates* are evaluated.

Two segments are added to this list if the distance between centers of mass of any of their rigid fragments is below a certain cutoff. This allows neighbors to be selected on a criterion of minimum distance of approach

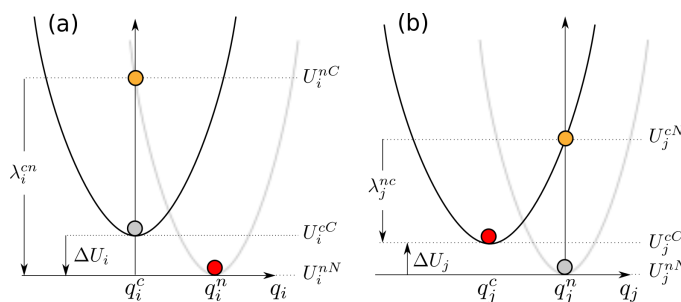


Figure 2.3: Potential energy surfaces of (a) donor and (b) acceptor in charged and neutral states. After the change of the charge state both molecules relax their nuclear coordinates. If all vibrational modes are treated classically, the total internal reorganization energy and the internal energy difference of the electron transfer reaction are $\lambda_{ij}^{\text{int}} = \lambda_i^{\text{cn}} + \lambda_j^{\text{nc}}$ and $\Delta E_{ij}^{\text{int}} = \Delta U_i - \Delta U_j$, respectively.

fig:parabolas

rather than center of mass distance, which is useful for molecules with anisotropic shapes.
 The neighbor list can be generated from the atomistic trajectory by using the `neighborlist` calculator.
 This calculator requires a cutoff, which can be specified in the `options.xml` file. The list is saved to the
`state.sql` file: `xtp_run -o options.xml -f state.sql -e neighborlist`

2.5 Reorganization energy

sec:reorganization

The reorganization energy λ_{ij} takes into account the change in nuclear (and dielectric) degrees of freedom as the charge moves from donor i to acceptor j . It has two contributions: intramolecular, $\lambda_{ij}^{\text{int}}$, which is due to reorganization of nuclear coordinates of the two molecules forming the charge transfer complex, and intermolecular (outersphere), $\lambda_{ij}^{\text{out}}$, which is due to the relaxation of the nuclear coordinates of the environment. In what follows we discuss how these contributions can be calculated.

2.5.1 Intramolecular reorganization energy

sec:intramolecular

If intramolecular vibrational modes of the two molecules are treated classically, the rearrangement of their nuclear coordinates after charge transfer results in the dissipation of the internal reorganization energy, $\lambda_{ij}^{\text{int}}$. It can be computed from four points on the potential energy surfaces (PES) of both molecules in neutral and charged states, as indicated in figure 2.3.
 Adding the contributions due to discharging of molecule i and charging of molecule j yields [8]

$$\lambda_{ij}^{\text{int}} = \lambda_i^{\text{cn}} + \lambda_j^{\text{nc}} = U_i^{\text{nC}} - U_i^{\text{nN}} + U_j^{\text{cN}} - U_j^{\text{cC}}. \quad (2.1)$$

equ:lamdas

Here U_i^{nC} is the internal energy of the neutral molecule i in the geometry of its charged state (small n denotes the state and capital C the geometry). Similarly, U_j^{cN} is the energy of the charged molecule j in the geometry of its neutral state. Note that the PES of the donor and acceptor are not identical for chemically different compounds or for conformers of the same molecule. In this case $\lambda_i^{\text{cn}} \neq \lambda_j^{\text{cn}}$ and $\lambda_i^{\text{nc}} \neq \lambda_j^{\text{nc}}$. Thus $\lambda_{ij}^{\text{int}}$ is a property of the charge transfer complex, and not of a single molecule.

Intramolecular reorganization energies for discharging (λ^{cn}) and charging (λ^{nc}) of a molecule need to be determined using quantum-chemistry and given in `map.xml`. The values are written to the `state.sql` using the calculator `einternal` (see also `internal energy`): `xtp_run -o options.xml -f state.sql -e einternal`

2.5.2 Outersphere reorganization energy

sec:outersphere

During the charge transfer reaction, also the molecules outside the charge transfer complex reorient and polarize in order to adjust for changes in electric potential, resulting in the outersphere contribution to the

reorganization energy. $\lambda_{ij}^{\text{out}}$ is particularly important if charge transfer occurs in a polarizable environment. Assuming that charge transfer is much slower than electronic polarization but much faster than nuclear rearrangement of the environment, $\lambda_{ij}^{\text{out}}$ can be calculated from the electric displacement fields created by the charge transfer complex [?]

$$\lambda_{ij}^{\text{out}} = \frac{c_p}{2\epsilon_0} \int_{V^{\text{out}}} dV \left[\vec{D}_I(\vec{r}) - \vec{D}_F(\vec{r}) \right]^2, \quad (2.2) \quad \text{equ:lambda_outer1}$$

where ϵ_0 is the the permittivity of free space, $\vec{D}_{I,F}(\vec{r})$ are the electric displacement fields created by the charge transfer complex in the initial (charge on molecule i) and final (charge transferred to molecule j) states, V^{out} is the volume outside the complex, and $c_p = \frac{1}{\epsilon_{\text{opt}}} - \frac{1}{\epsilon_s}$ is the Pekar factor, which is determined by the low (ϵ_s) and high (ϵ_{opt}) frequency dielectric permittivities.

Eq. (2.2) can be simplified by assuming spherically symmetric charge distributions on molecules i and j with total charge e . Integration over the volume V^{out} outside of the two spheres of radii R_i and R_j centered on molecules i and j leads to the classical Marcus expression for the outersphere reorganization energy

$$\lambda_{ij}^{\text{out}} = \frac{c_p e^2}{4\pi\epsilon_0} \left(\frac{1}{2R_i} + \frac{1}{2R_j} - \frac{1}{r_{ij}} \right), \quad (2.3) \quad \text{equ:lambda_outer2}$$

where r_{ij} is the molecular separation. While eq. (2.3) captures the main physics, e.g. predicts smaller outer-sphere reorganization energies (higher rates) for molecules at smaller separations, it often cannot provide quantitative estimates, since charge distributions are rarely spherically symmetric.

Alternatively, the displacement fields can be constructed using the atomic partial charges. The difference of the displacement fields at the position of an atom b_k outside the charge transfer complex (molecule $k \neq i, j$) can be expressed as

$$\vec{D}_I(\vec{r}_{b_k}) - \vec{D}_F(\vec{r}_{b_k}) = \sum_{a_i} \frac{q_{a_i}^c - q_{a_i}^n}{4\pi} \frac{(\vec{r}_{b_k} - \vec{r}_{a_i})}{|\vec{r}_{b_k} - \vec{r}_{a_i}|^3} + \sum_{a_j} \frac{q_{a_j}^n - q_{a_j}^c}{4\pi} \frac{(\vec{r}_{b_k} - \vec{r}_{a_j})}{|\vec{r}_{b_k} - \vec{r}_{a_j}|^3}, \quad (2.4)$$

where $q_{a_i}^n$ ($q_{a_i}^c$) is the partial charge of atom a of the neutral (charged) molecule i in vacuum. The partial charges of neutral and charged molecules are obtained by fitting their values to reproduce the electrostatic potential of a single molecule (charged or neutral) in vacuum. Assuming a uniform density of atoms, the integration in eq. (2.2) can be rewritten as a density-weighted sum over all atoms excluding those of the charge transfer complex.

The remaining unknown needed to calculate $\lambda_{ij}^{\text{out}}$ is the Pekar factor, c_p . In polar solvents $\epsilon_s \gg \epsilon_{\text{opt}} \sim 1$ and c_p is of the order of 1. In most organic semiconductors, however, molecular orientations are fixed and therefore the low frequency dielectric permittivity is of the same order of magnitude as ϵ_{opt} . Hence, c_p is small and its value is very sensitive to differences in the permittivities.

Outersphere reorganization energies for all pairs of molecules in the **neighbor list** can be computed from the atomistic trajectory by using the **outersphere calculator**.

Two methods can be used to compute $\lambda_{ij}^{\text{out}}$. The first method uses the atomistic partial charges of neutral and charged molecules from files specified in **map.xml** and eq. (2.2). The Pekar factor c_p and a cutoff radius based on molecular centers of mass have to be specified in the **options.xml** file.

If this method is computationally prohibitive, $\lambda_{ij}^{\text{out}}$ can be computed using eq. (2.3), which assumes spherical charge distributions on the molecules. In this case the radii of these spheres are specified in **segments.xml**, while the Pekar factor c_p is given in the **options.xml** file and no cutoff radius is needed.

The outer sphere reorganization energies are saved to the **state.sql** file: **xtp_run -o options.xml -f state.sql -e outersphere**

2.6 Site energies

A charge transfer reaction between molecules i and j is driven by the site energy difference, $\Delta E_{ij} = E_i - E_j$. Since the transfer rate, ω_{ij} , depends exponentially on ΔE_{ij} (see eq. (2.31)) it is important to compute its distribution as accurately as possible. The total site energy difference has contributions

205 due to *externally applied electric field, electrostatic interactions*, polarization effects, and *internal energy*
 206 differences. In what follows we discuss how to estimate these contributions by making use of first-principles
 207 calculations and polarizable force-fields.

208 2.6.1 Externally applied electric field

sec:ext_field

209 The contribution to the total site energy difference due to an external electric field \vec{F} is given by $\Delta E_{ij}^{\text{ext}} =$
 210 $q\vec{F} \cdot \vec{r}_{ij}$, where $q = \pm e$ is the charge and $\vec{r}_{ij} = \vec{r}_i - \vec{r}_j$ is a vector connecting molecules i and j . For typical
 211 distances between small molecules, which are of the order of 1 nm, and moderate fields of $F < 10^8$ V/m
 212 this term is always smaller than 0.1 eV.

213 2.6.2 Internal energy

sec:internal_energy

214 The contribution to the site energy difference due to different internal energies (see figure 2.3) can be
 215 written as

$$\Delta E_{ij}^{\text{int}} = \Delta U_i - \Delta U_j = (U_i^{cC} - U_i^{nN}) - (U_j^{cC} - U_j^{nN}), \quad (2.5) \quad \text{equ:conformational}$$

216 where $U_i^{cC(nN)}$ is the total energy of molecule i in the charged (neutral) state and geometry. ΔU_i cor-
 217 responds to the adiabatic ionization potential (or electron affinity) of molecule i , as shown in figure 2.3.
 218 For one-component systems and negligible conformational changes $\Delta E_{ij}^{\text{int}} = 0$, while it is significant for
 219 donor-acceptor systems.

220 Internal energies determined using quantum-chemistry need to be specified in `map.xml`. The values
 221 are written to the `state.sql` using the calculator `einternal` (see also *intramolecular reorganization*
 222 *energy*): `xtp_run -o options.xml -f state.sql -e einternal`

223 2.6.3 Electrostatic interaction energy

sec:distributed_multipoles

We represent the molecular charge density by choosing multiple expansion sites (“polar sites”) per molecule in such a way as to accurately reproduce the molecular electrostatic potential (ESP), with a set of suitably chosen multipole moments $\{Q_{lk}^a\}$ (in spherical-tensor notation) allocated to each site. The expression for the electrostatic interaction energy between two molecules A and B in the multi-point expansion includes an implicit sum over expansion sites $a \in A$ and $b \in B$,

$$U_{AB} = \sum_{a \in A} \sum_{b \in B} \hat{Q}_{l_1 k_1}^a T_{l_1 k_1 l_2 k_2}^{a,b} \hat{Q}_{l_2 k_2}^b \equiv \hat{Q}_{l_1 k_1}^a T_{l_1 k_1 l_2 k_2}^{a,b} \hat{Q}_{l_2 k_2}^b, \quad (2.6) \quad \text{equ:mol_distributed_U}$$

224 where we have used the Einstein sum convention for the site indices a and b on the right-hand side of the
 225 equation, in addition to the sum convention that is in place for the multipole-moment components $t \equiv l_1 k_1$
 226 and $u \equiv l_2 k_2$. The $T_{l_1 k_1 l_2 k_2}^{a,b}$ are tensors that mediate the interaction between a multipole component $l_1 k_1$
 227 on site a with the moment $l_2 k_2$ on site b . If we include the molecular environment into a perturbative term
 228 W to enter in the single-molecule Hamiltonian, the above expression is exactly the first-order correction to
 229 the energy where the quantum-mechanical detail has been absorbed in classical multipole moments.

230 There are a number of strategies how to arrive at such a collection of distributed multipoles. They can be
 231 classified according to whether the multipoles are derived (a) from the electrostatic potential generated by
 232 the SCF charge density or (b) from a decomposition of the wavefunction itself. Here, we will only draft two
 233 of those approaches, CHELPG [9] from category (a) and DMA [10] from category (b).

The CHELPG (CHarges from ELEctrostatic Potentials, Grid-based) method relies on performing a least-squares fit of atom-placed charges to reproduce the electrostatic potential as evaluated from the SCF density on a regularly spaced grid [9]. The fitted charges result from minimizing the Lagrangian function [11]

$$z(\{q_i\}) = \sum_{k=1}^M \left(\phi(\vec{r}_k) - \sum_{i=1}^N \frac{1}{4\pi\epsilon_0} \frac{q_i}{|\vec{r}_i - \vec{r}_k|} \right) + \lambda \left(q_{\text{mol}} - \sum_{i=1}^N q_i \right), \quad (2.7)$$

with M grid points, N atomic sites, the set of atomic partial charges $\{q_i\}$ and the SCF potential ϕ . The Lagrange multiplier λ constrains the sum of the fitted charges to the molecular charge q_{mol} . The main difference from other fitting schemes [12] is the algorithm that selects the positions at which the potential is evaluated (we note that the choice of grid points can have substantial effects especially for bulky molecules). Clearly, the CHELPG method can be (and has been) extended to include higher atomic multipoles. It should be noted, however, how already the inclusion of atomic dipoles hardly improves the parametrization, and can in fact be harmful to its conformational stability.

The Distributed-Multipole-Analysis (DMA) approach [10, 13], developed by A. Stone, operates directly on the quantum-mechanical density matrix, expanded in terms of atom- and bond-centered Gaussian functions $\chi_\alpha = R_{LK}(\vec{x} - \vec{s}_\alpha) \exp[-\zeta(\vec{x} - \vec{s}_\alpha)^2]$,

$$\rho(\vec{x}) = \sum_{\alpha, \beta} \rho_{\alpha\beta} \chi_\alpha(\vec{x} - \vec{s}_\alpha) \chi_\beta(\vec{x} - \vec{s}_\beta). \quad (2.8)$$

The aim is to compute multipole moments according in a distributed fashion: If we use that the overlap product $\chi_\alpha \chi_\beta$ of two Gaussian basis functions yields itself a Gaussian centered at $\vec{P} = (\zeta_\alpha \vec{s}_\alpha + \zeta_\beta \vec{s}_\beta) / (\zeta_\alpha + \zeta_\beta)$, it is possible to proceed in two steps: First, we compute the multipole moments associated with a specific summand in the density matrix, referred to the overlap center \vec{P} :

$$Q_{LK}[\vec{P}] = - \int R_{LK}(\vec{x} - \vec{P}) \rho_{\alpha\beta} \chi_\alpha \chi_\beta d^3x. \quad (2.9)$$

Second, we transfer the resulting $Q_{lk}[\vec{P}]$ to the position \vec{S} of a polar site according to the rule [10]

$$Q_{nm}[\vec{S}] = \sum_{l=0}^L \sum_{k=-l}^l \left[\binom{n+m}{l+k} \binom{n-m}{l-k} \right]^{1/2} R_{n-l, m-k}(\vec{S} - \vec{P}) \cdot Q_{lk}[\vec{P}]. \quad (2.10)$$

Note how this requires a rule for the choice of the expansion site to which the multipole moment should be transferred. In the near past [13], the nearest-site algorithm, which allocates the multipole moments to the site closest to the overlap center, was replaced for diffuse functions by an algorithm based on a sxtph weighting function in conjunction with grid-based integration methods in order to decrease the basis-set dependence of the resulting set of distributed multipoles.

One important advantage of the DMA approach over fitting algorithms such as CHELPG or Merz-Kollman (MK) is that higher-order moments can also be derived without too large an ambiguity.

The ‘mps’ file format used by VOTCA for the definition of distributed multipoles (as well as point polarizabilities, see subsequent section) is based on the GDMA punch format of A. Stone’s GDMA program [13] (the punch output file can be immediately plugged into VOTCA without any conversions to be applied). Furthermore the log-file of different QM packages (currently Gaussian, Turbomole and NWChem) may be fed into the `log2mps` tool, which will subsequently generate the appropriate mps-file.

`xtp_tools -o options.xml -e log2mps`

2.6.4 Induction energy - the Thole model

If we in addition to the permanent set of multipole moments $\{Q_t^a\}$ allow for induced moments $\{\Delta Q_t^a\}$ and penalize their generation with a bilinear form (giving rise to a strictly positive contribution to the energy),

$$U_{\text{int}} = \frac{1}{2} \sum_A \Delta Q_t^a \eta_{tt'}^{aa'} \Delta Q_{t'}^{a'}, \quad (2.11)$$

it can be shown that the induction contribution to the site energy evaluates to an expression where all interactions between induced moments have cancelled out, and interactions between permanent and induced moments are scaled down by 1/2 [14]:

$$U_{\text{pu}} = \frac{1}{2} \sum_A \sum_{B>A} [\Delta Q_t^a T_{tu}^{ab} Q_u^b + \Delta Q_t^b T_{tu}^{ab} Q_u^a]. \quad (2.12)$$

equu_pu

This term can be viewed as the second-order (induction) correction to the molecular interaction energy. The sets of $\{Q_t^a\}$ are solved for self-consistently via

$$\Delta Q_t^a = - \sum_{B \neq A} \alpha_{tt'}^{aa'} T_{t'u}^{a'b} (Q_u^b + \Delta Q_u^b), \quad (2.13) \quad \text{equ:self_consistent_dQ}$$

where the polarizability tensors $\alpha_{tt'}^{aa'}$ are given by the inverse of $\eta_{tt'}^{aa'}$. With eqs. 2.13 and 2.12 we have at hand expressions that allow us to compute the induction energy contribution to site energies in an iterative manner based on a set of molecular distributed multipoles $\{Q_t^a\}$ and polarizabilities $\{\alpha_{tt'}^{aa'}\}$. We have drafted in the previous section how to obtain the former from a wavefunction decomposition or fitting scheme (GDMA, CHELPG). The $\{\alpha_{tt'}^{aa'}\}$ can be derived formally (or rather: read off) from a perturbative expansion of the molecular interaction. In this work we make use of the Thole model [15?] as a semi-empirical approach to obtain the sought-after point polarizabilities in the local dipole approximation, that is, $[\alpha_{tt'}^{aa'}] = \alpha_{tt'}^{aa'} \delta_{t\beta} \delta_{t'\beta'} \delta_{aa'}$, where $\beta \in \{x, y, z\}$ references the dipole-moment component.

The Thole model is based on a modified dipole-dipole interaction, which can be reformulated in terms of the interaction of smeared charge densities. This has been shown to be necessary due to the divergent head-to-tail dipole-dipole interaction that otherwise results at small interseparations on the Å scale [15? ?]. Smearing out the charge distribution mimics the nature of the QM wavefunction, which effectively guards against this unphysical polarization catastrophe. Since the point dipoles however only react individually to the external field, any correlation effects as were still accounted for in the $\{\alpha_{tt'}^{aa'}\}$ are lost, except perhaps those correlations that are due to the mere classical field interaction.

The smearing of the nuclei-centered multipole moments is obtained via a fractional charge density $\rho_f(\vec{u})$ which should be normalized to unity and fall off rapidly as of a certain radius $\vec{u} = \vec{u}(\vec{R})$. The latter is related to the physical distance vector \vec{R} connecting two interacting sites via a linear scaling factor that takes into account the magnitude of the isotropic site polarizabilities α^a . This isotropic fractional charge density gives rise to a modified potential

$$\phi(u) = -\frac{1}{4\pi\epsilon_0} \int_0^u 4\pi u' \rho(u') du' \quad (2.14) \quad \text{equ:mod_potential}$$

We can relate the multipole interaction tensor $T_{ij\dots}$ (this time in Cartesian coordinates) to the fractional charge density in two steps: First, we rewrite the tensor in terms of the scaled distance vector \vec{u} ,

$$T_{ij\dots}(\vec{R}) = f(\alpha^a \alpha^b) t_{ij\dots}(\vec{u}(\vec{R}), \alpha^a \alpha^b), \quad (2.15)$$

where the specific form of $f(\alpha^a \alpha^b)$ results from the choice of $u(\vec{R}, \alpha^a \alpha^b)$. Second, we demand that the smeared interaction tensor $t_{ij\dots}$ is given as usual by the appropriate derivative of the potential in eq. 2.14,

$$t_{ij\dots}(\vec{u}) = -\partial_{u_i} \partial_{u_j} \dots \phi(\vec{u}). \quad (2.16)$$

It turns out that for a suitable choice of $\rho_f(\vec{u})$, the modified interaction tensors can be rewritten in such a way that powers n of the distance $R = |\vec{R}|$ are damped with a damping function $\lambda_n(\vec{u}(\vec{R}))$ [16].

There is a large number of fractional charge densities $\rho_f(\vec{u})$ that have been tested for the purpose of giving best results for the molecular polarizability as well as interaction energies. Note how a great advantage of the Thole model is the exceptional transferability of the atomic polarizabilities to compounds not used for the fitting procedure [?]. In fact, for most organic molecules, a fixed set of atomic polarizabilities ($\alpha_C = 1.334$, $\alpha_H = 0.496$, $\alpha_N = 1.073$, $\alpha_O = 0.873$, $\alpha_S = 2.926 \text{ Å}^3$) based on atomic elements yields satisfactory results.

VOTCA implements the Thole model with an exponentially-decaying fractional charge density

$$\rho(u) = \frac{3a}{4\pi} \exp(-au^3), \quad (2.17)$$

where $\vec{u}(\vec{R}, \alpha^a \alpha^b) = \vec{R}/(\alpha^a \alpha^b)^{1/6}$ and the smearing exponent $a = 0.39$ (which can however be changed from the program options), as used in the AMOEBA force field [16].

Even though the Thole model performs very well for many organic compounds with only the above small set of element-based polarizabilities, conjugated molecules may require a more intricate parametrization. The simplest approach is to resort to scaled polarizabilities to match the effective molecular polarizable volume $V \sim \alpha_x \alpha_y \alpha_z$ as predicted by QM calculations (here $\alpha_x, \alpha_y, \alpha_z$ are the eigenvalues of the molecular polarizability tensor). The `molpol` tool assists with this task, it self-consistently calculates the Thole polarizability for an input mps-file and optimizes (if desired) the atomic polarizabilities in the above simple manner.

```
xtp_tools -o options.xml -e molpol
```

The electrostatic and induction contribution to the site energy is evaluated by the `emultipole` calculator. Atomistic partial charges for charged and neutral molecules are taken from mps-files (extended GDMA format) specified in `map.xml`. Note that, in order to speed up calculations for both methods, a cut-off radius (for the molecular centers of mass) can be given in `options.xml`. Threaded execution is advised.

```
xtp_run -o options.xml -f state.sql -e emultipole
```

Furthermore available are `zmultipole`, which extends `emultipole` to allow for an electrostatic buffer layer (loosely related to the z-buffer in OpenGL, hence the name) and anisotropic point polarizabilities. For the interaction energy of charged clusters of any user-defined composition (Frenkel states, CT states, ...), `xqmultipole` can be used.

```
xtp_parallel -o options.xml -f state.sql -e xqmultipole
```

2.7 Transfer integrals

sec:transfer_integrals

The electronic transfer integral element J_{ij} entering the Marcus rates in eq. (2.31) is defined as

$$J_{ij} = \langle \phi_i | \hat{H} | \phi_j \rangle, \quad (2.18) \quad \text{equ:TI}$$

where ϕ_i and ϕ_j are diabatic wavefunctions, localized on molecule i and j respectively, participating in the charge transfer, and \hat{H} is the Hamiltonian of the formed dimer. Within the frozen-core approximation, the usual choice for the diabatic wavefunctions ϕ_i is the highest occupied molecular orbital (HOMO) in case of hole transport, and the lowest unoccupied molecular orbital (LUMO) in the case of electron transfer, while \hat{H} is an effective single particle Hamiltonian, e.g. Fock or Kohn-Sham operator of the dimer. As such, J_{ij} is a measure of the strength of the electronic coupling of the frontier orbitals of monomers mediated by the dimer interactions.

Intrinsically, the transfer integral is very sensitive to the molecular arrangement, i.e. the distance and the mutual orientation of the molecules participating in charge transport. Since this arrangement can also be significantly influenced by static and/or dynamic disorder [17? ? –19], it is essential to calculate J_{ij} explicitly for each hopping pair within a realistic morphology. Considering that the number of dimers for which eq. (2.18) has to be evaluated is proportional to the number of molecules times their coordination number, computationally efficient and at the same time quantitatively reliable schemes are required.

2.7.1 Projection of monomer orbitals on dimer orbitals (DIPRO)

sec:dipro

An approach for the determination of the transfer integral that can be used for any single-particle electronic structure method (Hartree-Fock, DFT, or semiempirical methods) is based on the projection of monomer orbitals on a manifold of explicitly calculated dimer orbitals. This dimer projection (DIPRO) technique including an assessment of computational parameters such as the basis set, exchange-correlation functionals, and convergence criteria is presented in detail in ref. [20]. A brief summary of the concept is given below. We start from an effective Hamiltonian ¹

$$\hat{H}^{\text{eff}} = \sum_i \epsilon_i \hat{a}_i^\dagger \hat{a}_i + \sum_{j \neq i} J_{ij} \hat{a}_i^\dagger \hat{a}_j + c.c. \quad (2.19) \quad \text{equ:dipro_eq1}$$

¹we use following notations: a - number, \vec{a} - vector, \mathbf{A} - matrix, \hat{A} - operator

where \hat{a}_i^\dagger and \hat{a}_i are the creation and annihilation operators for a charge carrier located at the molecular site i . The electron site energy is given by ϵ_i , while J_{ij} is the transfer integral between two sites i and j . We label their frontier orbitals (HOMO for hole transfer, LUMO for electron transfer) ϕ_i and ϕ_j , respectively. Assuming that the frontier orbitals of a dimer (adiabatic energy surfaces) result exclusively from the interaction of the frontier orbitals of monomers, and consequently expand them in terms of ϕ_i and ϕ_j . The expansion coefficients, $\bar{\mathbf{C}}$, can be determined by solving the secular equation

$$(\mathbf{H} - E\mathbf{S})\bar{\mathbf{C}} = 0 \quad (2.20) \quad \text{eq:dipro_eq2}$$

where \mathbf{H} and \mathbf{S} are the Hamiltonian and overlap matrices of the system, respectively. These matrices can be written explicitly as

$$\mathbf{H} = \begin{pmatrix} e_i & H_{ij} \\ H_{ij}^* & e_j \end{pmatrix} \quad \mathbf{S} = \begin{pmatrix} 1 & S_{ij} \\ S_{ij}^* & 1 \end{pmatrix} \quad (2.21) \quad \text{eq:dipro_eq3}$$

with

$$\begin{aligned} e_i &= \langle \phi_i | \hat{H} | \phi_i \rangle & H_{ij} &= \langle \phi_i | \hat{H} | \phi_j \rangle \\ e_j &= \langle \phi_j | \hat{H} | \phi_j \rangle & S_{ij} &= \langle \phi_j | \phi_i \rangle \end{aligned} \quad (2.22) \quad \text{eq:dipro_eq4}$$

The matrix elements $e_{i(j)}$, H_{ij} , and S_{ij} entering eq. (2.21) can be calculated via projections on the dimer orbitals (eigenfunctions of \hat{H}) $\{|\phi_n^D\rangle\}$ by inserting $\hat{1} = \sum_n |\phi_n^D\rangle \langle \phi_n^D|$ twice. We exemplify this explicitly for H_{ij} in the following

$$H_{ij} = \sum_{nm} \langle \phi_i | \phi_n^D \rangle \langle \phi_n^D | \hat{H} | \phi_m^D \rangle \langle \phi_m^D | \phi_j \rangle. \quad (2.23) \quad \text{eq:dipro_eq16}$$

The Hamiltonian is diagonal in its eigenfunctions, $\langle \phi_n^D | \hat{H} | \phi_m^D \rangle = E_n \delta_{nm}$. Collecting the projections of the frontier orbitals $|\phi_{i(j)}\rangle$ on the n -th dimer state $(\bar{\mathbf{V}}_{(i)})_n = \langle \phi_i | \phi_n^D \rangle$ and $(\bar{\mathbf{V}}_{(j)})_n = \langle \phi_j | \phi_n^D \rangle$ respectively, into vectors we obtain

$$H_{ij} = \bar{\mathbf{V}}_{(i)} \mathbf{E} \bar{\mathbf{V}}_{(j)}^\dagger. \quad (2.24) \quad \text{eq:dipro_eq17}$$

What is left to do is determine these projections $\bar{\mathbf{V}}_{(k)}$. In all practical calculations the molecular orbitals are expanded in basis sets of either plane waves or of localized atomic orbitals $|\varphi_\alpha\rangle$. We will first consider the case that the calculations for the monomers are performed using a counterpoise basis set that is commonly used to deal with the basis set superposition error (BSSE). The basis set of atom-centered orbitals of a monomer is extended to the one of the dimer by adding the respective atomic orbitals at virtual coordinates of the second monomer. We can then write the respective expansions as

$$|\phi_k\rangle = \sum_\alpha \lambda_\alpha^{(k)} |\varphi_\alpha\rangle \quad \text{and} \quad |\phi_n^D\rangle = \sum_\alpha D_\alpha^{(n)} |\varphi_\alpha\rangle \quad (2.25) \quad \text{eq:dipro_eq18}$$

where $k = i, j$. The projections can then be determined within this common basis set as

$$(\bar{\mathbf{V}}_k)_n = \langle \phi_k | \phi_n^D \rangle = \sum_\alpha \lambda_\alpha^{(k)} \langle \alpha | \sum_\beta D_\beta^{(n)} | \beta \rangle = \bar{\lambda}_{(k)}^\dagger \mathbf{S} \bar{\mathbf{D}}_{(n)} \quad (2.26) \quad \text{eq:dipro_eq19}$$

where \mathbf{S} is the overlap matrix of the atomic basis functions. This allows us to finally write the elements of the Hamiltonian and overlap matrices in eq. (2.21) as:

$$\begin{aligned} H_{ij} &= \bar{\lambda}_{(i)}^\dagger \mathbf{S} \mathbf{E} \mathbf{D}^\dagger \mathbf{S}^\dagger \bar{\lambda}_{(j)} \\ S_{ij} &= \bar{\lambda}_{(i)}^\dagger \mathbf{S} \mathbf{D} \mathbf{D}^\dagger \mathbf{S}^\dagger \bar{\lambda}_{(j)} \end{aligned} \quad (2.27) \quad \text{eq:dipro_eq20}$$

Since the two monomer frontier orbitals that form the basis of this expansion are not orthogonal in general ($\mathbf{S} \neq \mathbf{1}$), it is necessary to transform eq. (2.20) into a standard eigenvalue problem of the form

$$\mathbf{H}^{\text{eff}} \bar{\mathbf{C}}^{\text{eff}} = E \bar{\mathbf{C}}^{\text{eff}} \quad (2.28) \quad \text{eq:dipro_eq7}$$

347 to make it correspond to eq. (2.19). According to Löwdin such a transformation can be achieved by

$$\mathbf{H}^{\text{eff}} = \mathbf{S}^{-1/2} \mathbf{H} \mathbf{S}^{-1/2}. \quad (2.29) \quad \text{eq:dipro_eq9}$$

348 This then yields an effective Hamiltonian matrix in an orthogonal basis, and its entries can directly be
 349 identified with the site energies ϵ_i and transfer integrals J_{ij} :

$$\mathbf{H}^{\text{eff}} = \begin{pmatrix} e_i^{\text{eff}} & H_{ij}^{\text{eff}} \\ H_{ij}^{*,\text{eff}} & e_j^{\text{eff}} \end{pmatrix} = \begin{pmatrix} \epsilon_i & J_{ij} \\ J_{ij}^* & \epsilon_j \end{pmatrix} \quad (2.30) \quad \text{eq:dipro_eq11}$$

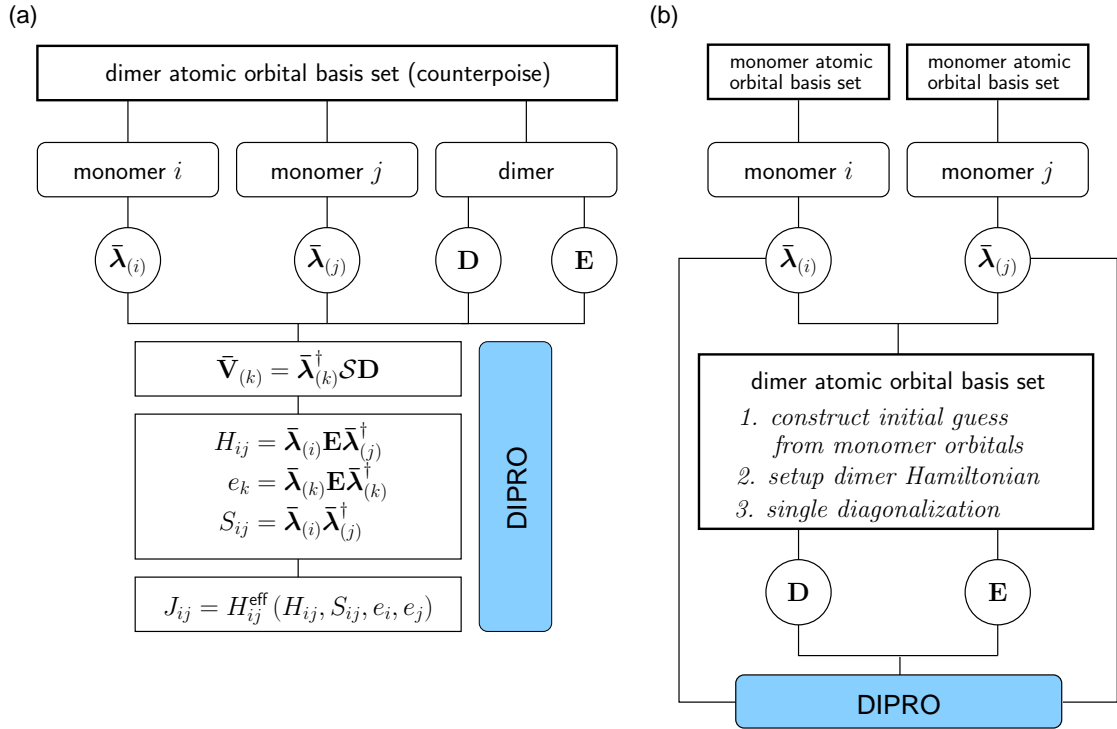


Figure 2.4: Schematics of the DIPRO method. (a) General workflow of the projection technique. (b) Strategy of the efficient noCP+noSCF implementation, in which the monomer calculations are performed independently from the dimer configurations (noCP), using the `edft` calculator. The dimer Hamiltonian is subsequently constructed based on an initial guess formed from monomer orbitals and only diagonalized once (noSCF) before the transfer integral is calculated by projection. This second step is performed by the `idft` calculator.

fig:dipro_scheme

2.7.2 DFT-based transfer integrals using DIPRO

350

sec:dft

351

352

353

354

355

356

357

358

The calculation of one electronic coupling element based on DFT using the DIPRO method requires the overlap matrix of atomic orbitals \mathbf{S} , the expansion coefficients for monomer $\bar{\lambda}_{(k)} = \{\lambda_{\alpha}^{(k)}\}$ and dimer orbitals $\bar{\mathbf{D}}_{(n)} = \{D_{\alpha}^{(n)}\}$, as well as the orbital energies E_n of the dimer are required as input. In practical situations, performing self-consistent quantum-chemical calculations for each individual monomer and one for the dimer to obtain this input data is extremely demanding. Several simplifications can be made to reduce the computational effort, such as using non-Counterpoise basis sets for the monomers (thereby decoupling the monomer calculations from the dimer run) and performing only a single SCF step in a dimer calculation starting from an initial guess formed from a superposition of monomer orbitals. This

359 "noCP+noSCF" variant of DIPRO is shown in figure 2.4(a) and recommended for production runs. A
 360 detailed comparative study of the different variants can be found in [20].
 361 The code currently contains supports evaluation of transfer integrals from quantum-chemical calculations
 362 performed with the Gaussian, Turbomole, and NWChem packages. The interfacing procedure consists
 363 of three main steps: generation of input files for monomers and dimers, performing the actual quantum-
 364 chemical calculations, and calculating the transfer integrals.

365 Monomer calculations

sec:edft

366 First, *hopping sites* and a *neighbor list* need to be generated from the atomistic topology and trajectory and
 367 written to the `state.sql` file. Then the parallel *edft calculator* manages the calculation of the monomer
 368 properties required for the determination of electronic coupling elements. Specifically, the individual steps
 369 it performs are:

- 370 1. Creation of a job file containing the list of molecules to be calculated with DFT `xtp_parallel -o`
 371 `options.xml -f state.sql -e edft -j write`
- 372 2. Running of all jobs in job file `xtp_parallel -o options.xml -f state.sql -e edft -j`
 373 `run` which includes
 - 374 • creating the input files for the DFT calculation (using the package specified in `options.xml`)
 375 in the directory
 376 `OR_FILES/package/frame_F/mol_M`
 377 where `F` is the index of the frame in the trajectory, `M` is the index of a molecule in this frame,
 - 378 • executing the DFT run, and
 - 379 • after completion of this run, parsing the output (number of electrons, basis set, molecular
 380 orbital expansion coefficients), and saving it in compressed form to
 381 `OR_FILES/molecules/frame_F/molecule_M.orb`

382 Calculating the transfer integrals

sec:edft

383 After the monomer calculations have been completed successfully, the respective runs for dimers from the
 384 neighborlist can be performed using the parallel *idft calculator*, which manages the DFT runs for the
 385 hopping pairs and determines the coupling element using DIPRO. Again, several steps are required:

- 386 1. Creation of a job file containing the list of pairs to be calculated with DFT `xtp_parallel -o`
 387 `options.xml -f state.sql -e idft -j write`
- 388 2. Running of all jobs in job file `xtp_parallel -o options.xml -f state.sql -e idft -j`
 389 `run` which includes
 - 390 • creating the input files (including the merged guess for a noSCF calculation, if requested) for
 391 the DFT calculation (using the package specified in `options.xml`) in the directory
 392 `OR_FILES/package/frame_F/pair_M_N`
 393 where `M` and `N` are the indices of the molecules in this pair,
 - 394 • executing the DFT run, and
 - 395 • after completion of this run, parsing the output (number of electrons, basis set, molecular
 396 orbital expansion coefficients and energies, atomic orbital overlap matrix), and saving the pair
 397 information in compressed form to
 398 `OR_FILES/pairs/frame_F/pair_M_N.orb`
 - 399 • loading the monomer orbitals from the previously saved `*.orb` files.

- calculating the coupling elements and write them to the job file
3. Reading the coupling elements from the job file and saving them to the `state.sql` file `xtp_parallel`
`-o options.xml -f state.sql -e idft -j read`

2.7.3 ZINDO-based transfer integrals using MOO

sec:zindo

An approximate method based on Zerner's Intermediate Neglect of Differential Overlap (ZINDO) has been described in Ref. [21]. This semiempirical method is substantially faster than first-principles approaches, since it avoids the self-consistent calculations on each individual monomer and dimer. This allows to construct the matrix elements of the ZINDO Hamiltonian of the dimer from the weighted overlap of molecular orbitals of the two monomers. Together with the introduction of rigid segments, only a single self-consistent calculation on one isolated conjugated segment is required. All relevant molecular overlaps can then be constructed from the obtained molecular orbitals.

The main advantage of the molecular orbital overlap (MOO) library is fast evaluation of electronic coupling elements. Note that MOO is based on the ZINDO Hamiltonian which has limited applicability. The general advice is to first compare the accuracy of the MOO method to the DFT-based calculations.

MOO can be used both in a `standalone mode` and as an `izindo calculator` of VOTCA-XTP.

Since MOO constructs the Fock operator of a dimer from the molecular orbitals of monomers by translating and rotating the orbitals of `rigid fragments`, the optimized geometry of all `conjugated segments` and the coefficients of the molecular orbitals are required as its input in addition to the state file (`state.sql`) with the `neighbor list`. Coordinates are stored in `geometry.xyz` files with four columns, first being the atom type and the next three atom coordinates. This is a standard xyz format without a header. Note that the atom order in the `geometry.xyz` files can be different from that of the mapping files. The correspondence between the two is established in the `map.xml` file.

Izindo requires the specification of orbitals for hole and electron transport in `map.xml`. They are the HOMO and LUMO respectively and can be retrieved from the log file from which the `zindo.orb` file is generated. The number of alpha electrons is the HOMO, the LUMO is HOMO+1

The calculated transfer integrals are immediately saved to the `state.sql` file. `xtp_run -o options.xml -f state.sql -e izindo`

2.8 Charge transfer rate

sec:rates

Charge transfer rates can be postulated based on intuitive physical considerations, as it is done in the Gaussian disorder models [22–25]. Alternatively, charge transfer theories can be used to evaluate rates from quantum chemical calculations [1, 8, 20, 26–28]. In spite of being significantly more computationally demanding, the latter approach allows to link the chemical and electronic structure, as well as the morphology, to charge dynamics.

2.8.1 Classical charge transfer rate

sec:rate_classical

The high temperature limit of classical charge transfer theory [29, 30] is often used as a trade-off between theoretical rigor and computational complexity. It captures key parameters which influence charge transport while at the same time providing an analytical expression for the rate. Within this limit, the transfer rate for a charge to hop from a site i to a site j reads

$$\omega_{ij} = \frac{2\pi}{\hbar} \frac{J_{ij}^2}{\sqrt{4\pi\lambda_{ij}k_B T}} \exp \left[-\frac{(\Delta E_{ij} - \lambda_{ij})^2}{4\lambda_{ij}k_B T} \right], \quad (2.31) \quad \text{equ:marcus}$$

where T is the temperature, $\lambda_{ij} = \lambda_{ij}^{\text{int}} + \lambda_{ij}^{\text{out}}$ is the `reorganization energy`, which is a sum of intra- and inter-molecular (outersphere) contributions, ΔE_{ij} is the `site-energy difference`, or driving force, and J_{ij} is the `electronic coupling element`, or transfer integral.

2.8.2 Semi-classical bimolecular rate

The main assumptions in eq. (2.31) are non-adiabaticity (small electronic coupling and charge transfer between two diabatic, non-interacting states), and harmonic promoting modes, which are treated classically. At ambient conditions, however, the intramolecular promoting mode, which roughly corresponds to C-C bond stretching, has a vibrational energy of $\hbar\omega \approx 0.2 \text{ eV} \gg k_B T$ and should be treated quantum-mechanically. The outer-sphere (slow) mode has much lower vibrational energy than the intramolecular promoting mode, and therefore can be treated classically. The weak interaction between molecules also implies that each molecule has its own, practically independent, set of quantum mechanical degrees of freedom.

A more general, quantum-classical expression for a bimolecular multi-channel rate is derived in the Supporting Information of ref. [1] and has the following form

$$\omega_{ij} = \frac{2\pi}{\hbar} \frac{|J_{ij}|^2}{\sqrt{4\pi\lambda_{ij}^{\text{out}} k_B T}} \sum_{l', m'=0}^{\infty} |\langle \chi_{i0}^c | \chi_{il'}^n \rangle|^2 |\langle \chi_{j0}^n | \chi_{jm'}^c \rangle|^2 \exp \left\{ -\frac{[\Delta E_{ij} - \hbar(l'\omega_i^n + m'\omega_j^c) - \lambda_{ij}^{\text{out}}]^2}{4\lambda_{ij}^{\text{out}} k_B T} \right\}. \quad (2.32)$$

If the curvatures of intramolecular PES of charged and neutral states of a molecule are different, that is $\omega_i^c \neq \omega_i^n$, the corresponding reorganization energies, $\lambda_i^{cn} = \frac{1}{2}[\omega_i^n(q_i^n - q_i^c)]^2$ and $\lambda_i^{nc} = \frac{1}{2}[\omega_i^c(q_i^n - q_i^c)]^2$, will also differ. In this case the Franck-Condon (FC) factors for discharging of molecule i read [31]

$$|\langle \chi_{i0}^c | \chi_{il'}^n \rangle|^2 = \frac{2}{2^{l'} l'!} \frac{\sqrt{\omega_i^c \omega_i^n}}{(\omega_i^c + \omega_i^n)} \exp(-|s_i|) \left[\sum_{\substack{k=0 \\ k \text{ even}}}^{l'} \binom{l'}{k} \left(\frac{2\omega_i^c}{\omega_i^c + \omega_i^n} \right)^{k/2} \frac{k!}{(k/2)!} H_{l'-k} \left(\frac{s_i}{\sqrt{2S_i^{cn}}} \right) \right]^2, \quad (2.33)$$

where $H_n(x)$ is a Hermite polynomial, $s_i = 2\sqrt{\lambda_i^{nc}\lambda_i^{cn}}/\hbar(\omega_i^c + \omega_i^n)$, and $S_i^{cn} = \lambda_i^{cn}/\hbar\omega_i^c$. The FC factors for charging of molecule j can be obtained by substituting $(s_i, S_i^{cn}, \omega_i^c)$ with $(-s_j, S_j^{nc}, \omega_j^n)$. In order to evaluate the FC factors, the **internal reorganization energy** λ_i^{cn} can be computed from the intramolecular PES.

2.8.3 Semi-classical rate

One can also use the quantum-classical rate with a common set of vibrational coordinates [?]

$$\omega_{ij} = \frac{2\pi}{\hbar} \frac{|J_{ij}|^2}{\sqrt{4\pi\lambda_{ij}^{\text{out}} k_B T}} \sum_{N=0}^{\infty} \frac{1}{N!} \left(\frac{\lambda_{ij}^{\text{int}}}{\hbar\omega^{\text{int}}} \right)^N \exp \left(-\frac{\lambda_{ij}^{\text{int}}}{\hbar\omega^{\text{int}}} \right) \exp \left\{ -\frac{[\Delta E_{ij} - \hbar N\omega^{\text{int}} - \lambda_{ij}^{\text{out}}]^2}{4\lambda_{ij}^{\text{out}} k_B T} \right\}. \quad (2.34)$$

Numerical estimates show that if $\lambda_{ij}^{\text{int}} \approx \lambda_{ij}^{\text{out}}$ and $|\Delta E_{ij}| \ll \lambda_{ij}^{\text{out}}$ the rates are similar to those of eq. (2.31). In general, there is no robust method to compute $\lambda_{ij}^{\text{out}}$ [32] and both reorganization energies are often assumed to be of the same order of magnitude. In this case the second condition also holds, unless there are large differences in electron affinities or ionization potentials of neighboring molecules, e.g. in donor-acceptor blends.

To calculate rates of the type specified in `options.xml` for all pairs in the **neighbor list** and to save them into the `state.sql` file, run the **rates calculator**. Note that all required ingredients (**reorganization energies**, **transfer integrals**, and **site energies** have to be calculated before). `xtp_run -o options.xml -f state.sql -e rates`

2.9 Master equation

sec:kmc

Having determined the list of conjugated segments (hopping sites) and charge transfer rates between them, the next task is to solve the master equation which describes the time evolution of the system

$$\frac{\partial P_\alpha}{\partial t} = \sum_{\beta} P_\beta \Omega_{\beta\alpha} - \sum_{\beta} P_\alpha \Omega_{\alpha\beta}, \quad (2.35) \quad \text{equ:master}$$

where P_α is the probability of the system to be in a state α at time t and $\Omega_{\alpha\beta}$ is the transition rate from state α to state β . A state α is specified by a set of site occupations, $\{\alpha_i\}$, where $\alpha_i = 1(0)$ for an occupied (unoccupied) site i , and the matrix $\hat{\Omega}$ can be constructed from rates ω_{ij} .

The solution of eq. (2.35) is obtained by using kinetic Monte Carlo (KMC) methods. KMC explicitly simulates the dynamics of charge carriers by constructing a Markov chain in state space and can find both stationary and transient solutions of the master equation. The main advantage of KMC is that only states with a direct link to the current state need to be considered at each step. Since these can be constructed solely from current site occupations, extensions to multiple charge carriers (without the mean-field approximation), site-occupation dependent rates (needed for the explicit treatment of Coulomb interactions), and different types of interacting particles and processes, are straightforward. To optimize memory usage and efficiency, a combination of the variable step size method [33] and the first reaction method is implemented. To obtain the dynamics of charges using KMC, the program `xtp_kmc_run` executes a specific `calculator` after reading its options (charge carrier type, runtime, number of carriers etc.) from `options.xml`.

```
xtp_kmc_run -o options.xml -f state.sql -e kmcsingle
xtp_kmc_run -o options.xml -f state.sql -e kmcmultiple
```

2.9.1 Extrapolation to nondispersive mobilities

sec:nondispersive

Predictions of charge-carrier mobilities in partially disordered semiconductors rely on charge transport simulations in systems which are only several nanometers thick. As a result, simulated charge transport might be dispersive for materials with large energetic disorder [34, 35] and simulated mobilities are system-size dependent. In time-of-flight (TOF) experiments, however, a typical sample thickness is in the micrometer range and transport is often nondispersive. In order to link simulation and experiment, one needs to extract the nondispersive mobility from simulations of small systems, where charge transport is dispersive at room temperature.

Such extrapolation is possible if the temperature dependence of the nondispersive mobility is known in a wide temperature range. For example, one can use analytical results derived for one-dimensional models [36–38]. The mobility-temperature dependence can then be parametrized by simulating charge transport at elevated temperatures, for which transport is nondispersive even for small system sizes. This dependence can then be used to extrapolate to the nondispersive mobility at room temperature [39].

For Alq₃, the charge carrier mobility of a periodic system of 512 molecules was shown to be more than three orders of magnitude higher than the nondispersive mobility of an infinitely large system [39]. Furthermore, it was shown that the transition between the dispersive and nondispersive transport has a logarithmic dependence on the number of hopping sites N . Hence, a brute-force increase of the system size cannot resolve the problem for compounds with large energetic disorder σ , since N increases exponentially with σ^2 .

2.10 Macroscopic observables

sec:analysis

Spatial distributions of charge and current densities can provide a better insight in the microscopic mechanisms of charge transport. If O is an observable which has a value O_α in a state α , its ensemble average at time t is a sum over all states weighted by the probability P_α to be in a state α at time t

$$\langle O \rangle = \sum_{\alpha} O_{\alpha} P_{\alpha}. \quad (2.36) \quad \text{equ:ensemble}$$

507 If O does not explicitly depend on time, the time evolution of $\langle O \rangle$ can be calculated as

$$\frac{d\langle O \rangle}{dt} = \sum_{\alpha, \beta} [P_{\beta} \Omega_{\beta\alpha} - P_{\alpha} \Omega_{\alpha\beta}] O_{\alpha} = \sum_{\alpha, \beta} P_{\beta} \Omega_{\beta\alpha} [O_{\alpha} - O_{\beta}]. \quad (2.37)$$

508 If averages are obtained from KMC trajectories, $P_{\alpha} = s_{\alpha}/s$, where s_{α} is the number of Markov chains
509 ending in the state α after time t , and s is the total number of chains.

Alternatively, one can calculate time averages by analyzing a single Markov chain. If the total occupation time of the state α is τ_{α} then

$$\bar{O} = \frac{1}{\tau} \sum_{\alpha} O_{\alpha} \tau_{\alpha}, \quad (2.38) \quad \text{equ:time}$$

510 where $\tau = \sum_{\alpha} \tau_{\alpha}$ is the total time used for time averaging.

511 For ergodic systems and sufficient sampling times, ensemble and time averages should give identical re-
512 sults. In many cases, the averaging procedure reflects a specific experimental technique. For example, an
513 ensemble average over several KMC trajectories with different starting conditions corresponds to averag-
514 ing over injected charge carriers in a time-of-flight experiment. In what follows, we focus on the single
515 charge carrier (low concentration of charges) case.

516 2.10.1 Charge density

sec:occupation

517 For a specific type of particles, the microscopic charge density of a site i is proportional to the occupation
518 probability of the site, p_i

$$\rho_i = e p_i / V_i, \quad (2.39)$$

519 where, for an irregular lattice, the effective volume V_i can be obtained from a Voronoi tessellation of space.
520 For reasonably uniform lattices (uniform site densities) this volume is almost independent of the site and
521 a constant volume per site, $V_i = V/N$, can be assumed. In the macroscopic limit, the charge density can
522 be calculated using a sxtpting kernel function, i.e. a distance-weighted average over multiple sites. Site
523 occupations p_i can be obtained from eq. (2.36) or eq. (2.38) by using the occupation of site i in state α as
524 an observable.

525 If the system is in thermodynamic equilibrium, that is without sources or sinks and without circular
526 currents (and therefore no net flux) a condition, known as detailed balance, holds

$$p_j \omega_{ji} = p_i \omega_{ij}, \quad (2.40) \quad \text{equ:detailed_balance}$$

527 It can be used to test whether the system is ergodic or not by correlating $\log p_i$ and the site energy E_i .
528 Indeed, if $\lambda_{ij} = \lambda_{ji}$ the ratios of forward and backward rates are determined solely by the energetic disorder,
529 $\omega_{ji}/\omega_{ij} = \exp(-\Delta E_{ij}/k_B T)$ (see eq. (2.31)).

530 2.10.2 Current

sec:vaverage

531 If the position of the charge, \vec{r} , is an observable, the time evolution of its average $\langle \vec{r} \rangle$ is the total current in
532 the system

$$\vec{J} = e \langle \vec{v} \rangle = e \frac{d\langle \vec{r} \rangle}{dt} = e \sum_{i,j} p_j \omega_{ji} (\vec{r}_i - \vec{r}_j). \quad (2.41) \quad \text{equ:current_def}$$

533 Symmetrizing this expression we obtain

$$\vec{J} = \frac{1}{2} e \sum_{i,j} (p_j \omega_{ji} - p_i \omega_{ij}) \vec{r}_{ij}, \quad (2.42) \quad \text{equ:current}$$

534 where $\vec{r}_{ij} = \vec{r}_i - \vec{r}_j$. Symmetrization ensures equal flux splitting between neighboring sites and absence
535 of local average fluxes in equilibrium. It allows to define a local current through site i as

$$\vec{J}_i = \frac{1}{2} e \sum_j (p_j \omega_{ji} - p_i \omega_{ij}) \vec{r}_{ij}. \quad (2.43) \quad \text{equ:site_current}$$

A large value of the local current indicates that the site contributes considerably to the total current. A collection of such sites thus represents most favorable charge pathways [40].

2.10.3 Mobility and diffusion constant

For a single particle, e.g. a charge or an exciton, a zero-field mobility can be determined by studying particle diffusion in the absence of external fields. Using the particle displacement squared, Δr_i^2 , as an observable we obtain

$$2dD_{\gamma\delta} = \frac{d \langle \Delta r_{i,\gamma} \Delta r_{i,\delta} \rangle}{dt} = \sum_{\substack{i,j \\ i \neq j}} p_j \omega_{ji} (\Delta r_{i,\gamma} \Delta r_{i,\delta} - \Delta r_{j,\gamma} \Delta r_{j,\delta}) = \sum_{\substack{i,j \\ i \neq j}} p_j \omega_{ji} (r_{i,\gamma} r_{i,\delta} - r_{j,\gamma} r_{j,\delta}) . \quad (2.44)$$

Here \vec{r}_i is the coordinate of the site i , $D_{\gamma\delta}$ is the diffusion tensor, $\gamma, \delta = x, y, z$, and $d = 3$ is the system dimension. Using the Einstein relation,

$$D_{\gamma\delta} = k_B T \mu_{\gamma\delta} , \quad (2.45)$$

one can, in principle, obtain the zero-field mobility tensor $\mu_{\gamma\delta}$. Eq. (2.44), however, does not take into account the use of periodic boundary conditions when simulating charge dynamics. In this case, the simulated occupation probabilities can be compared to the solution of the Smoluchowski equation with periodic boundary conditions (see the supporting information for details).

Alternatively, one can directly analyze time-evolution of the KMC trajectory and obtain the diffusion tensor from a linear fit to the mean square displacement, $\Delta r_{i,\gamma} \Delta r_{i,\delta} = 2dD_{\gamma\delta}t$.

The charge carrier mobility tensor, $\hat{\mu}$, for any value of the external field can be determined either from the average charge velocity defined in eq. (2.41)

$$\langle \vec{v} \rangle = \sum_{i,j} p_j \omega_{ji} (\vec{r}_i - \vec{r}_j) = \hat{\mu} \vec{F} , \quad (2.46)$$

or directly from the KMC trajectory. In the latter case the velocity is calculated from the unwrapped (if periodic boundary conditions are used) charge displacement vector divided by the total simulation time. Projecting this velocity on the direction of the field \vec{F} yields the charge carrier mobility in this particular direction. In order to improve statistics, mobilities can be averaged over several KMC trajectories and MD snapshots.

2.10.4 Spatial correlations of energetic disorder

Long-range, e.g. electrostatic and polarization, interactions often result in spatially correlated disorder [41], which affects the onset of the mobility-field (Poole-Frenkel) dependence [36, 42, 43].

To quantify the degree of correlation, one can calculate the spatial correlation function of E_i and E_j at a distance r_{ij}

$$C(r_{ij}) = \frac{\langle (E_i - \langle E \rangle) (E_j - \langle E \rangle) \rangle}{\langle (E_i - \langle E \rangle)^2 \rangle} , \quad (2.47)$$

where $\langle E \rangle$ is the average site energy. $C(r_{ij})$ is zero if E_i and E_j are uncorrelated and 1 if they are fully correlated. For a system of randomly oriented point dipoles, the correlation function decays as $1/r$ at large distances [44].

For systems with spatial correlations, variations in site energy differences, ΔE_{ij} , of pairs of molecules from the neighbor list are smaller than variations in site energies, E_i , of all individual molecules. Since only neighbor list pairs affect transport, the distribution of ΔE_{ij} rather than that of individual site energies, E_i , should be used to characterize energetic disorder.

Note that the `eanalyze` calculator takes into account all contributions to the site energies `xtp_run -o options.xml -f state.sql -e eanalyze`

571

Chapter 3

572

Input and output files

sec:io

573

3.1 Atomistic topology

sec:atomistic

574

If you are using GROMACS for generating atomistic configurations, it is possible to directly use the topology file provided by GROMACS (`topology.tpr`). In this case the GROMACS residue and atom names should be used to specify the *coarse-grained topology* and *conjugated segments*.

575

576

577

578

579

580

581

582

A custom topology can also be defined using an XML file. Moreover, it is possible to partially overwrite the information provided in, for example, GROMACS topology file. We will illustrate how to create a custom topology file using DCV2T. The structure of DCV2T, together with atom type definitions, is shown in fig. 3.1. DCV2T has two thiophene (THI) and two dicyanovinyl (NIT) residues. The `pdb` file which contains residue types, residue numbering, atom names, atom types, and atom coordinates is shown in listing 3.1.

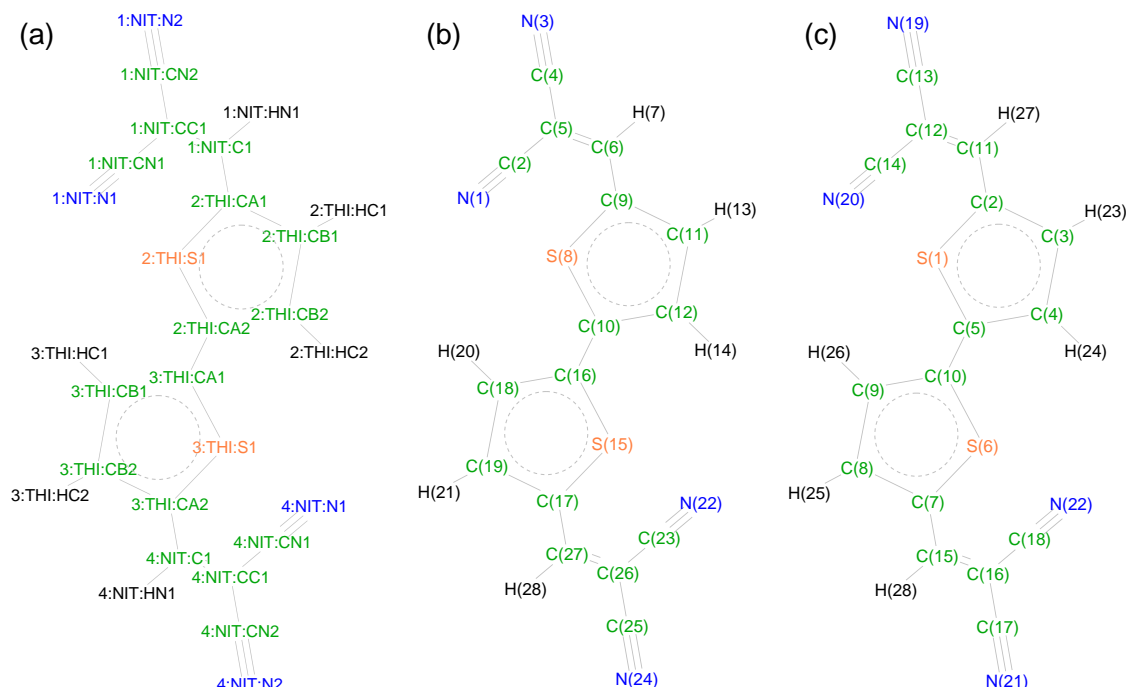


Figure 3.1: (a) DCV2T with atoms labelled according to `residue_number:residue_name:atom_name`. There are four residues and two residue types: thiophene (THI) and dicyanovinyl (NIT). The corresponding `pdb` file is shown in listing 3.1. Atom numbering is used to split conjugated segments on rigid fragments and to link atomistic ((b) from GROMACS topology) and quantum descriptions (c).

fig:dcv2t

list.pdb

Listing 3.1: pdb file of DCV2T.

583											
584	HETATM	1	N1	NIT	1	2.388	8.533	11.066	1.00	4.14	N
585	HETATM	2	CN1	NIT	1	1.984	9.553	10.718	1.00	2.54	C
586	HETATM	3	N2	NIT	1	-1.138	10.872	10.087	1.00	3.24	N
587	HETATM	4	CN2	NIT	1	0.003	10.871	10.213	1.00	2.37	C
588	HETATM	5	CC1	NIT	1	1.441	10.824	10.327	1.00	1.91	C
589	HETATM	6	C1	NIT	1	2.193	11.939	10.071	1.00	1.61	C
590	HETATM	7	HN1	NIT	1	1.715	12.710	9.872	1.00	1.97	H
591	HETATM	8	S1	THI	2	4.758	10.743	10.130	1.00	1.52	S
592	HETATM	9	CA1	THI	2	3.613	12.024	9.948	1.00	1.22	C
593	HETATM	10	CA2	THI	2	6.099	11.836	9.997	1.00	1.30	C
594	HETATM	11	CB1	THI	2	4.251	13.243	9.782	1.00	1.39	C
595	HETATM	12	CB2	THI	2	5.658	13.131	9.818	1.00	1.45	C
596	HETATM	13	HC1	THI	2	3.800	14.047	9.660	1.00	1.66	H
597	HETATM	14	HC2	THI	2	6.230	13.860	9.731	1.00	1.74	H
598	HETATM	15	S1	THI	3	8.803	12.414	9.882	1.00	1.38	S
599	HETATM	16	CA1	THI	3	7.456	11.347	10.094	1.00	1.37	C
600	HETATM	17	CA2	THI	3	9.940	11.122	10.152	1.00	1.42	C
601	HETATM	18	CB1	THI	3	7.873	10.048	10.355	1.00	1.73	C
602	HETATM	19	CB2	THI	3	9.267	9.926	10.399	1.00	1.82	C
603	HETATM	20	HC1	THI	3	7.288	9.335	10.487	1.00	2.05	H
604	HETATM	21	HC2	THI	3	9.704	9.123	10.576	1.00	2.21	H
605	HETATM	22	N1	NIT	4	11.235	14.572	9.094	1.00	3.08	N
606	HETATM	23	CN1	NIT	4	11.665	13.566	9.441	1.00	2.04	C
607	HETATM	24	N2	NIT	4	14.733	12.005	10.009	1.00	2.17	N
608	HETATM	25	CN2	NIT	4	13.590	12.149	9.933	1.00	1.77	C
609	HETATM	26	CC1	NIT	4	12.156	12.282	9.861	1.00	1.71	C
610	HETATM	27	C1	NIT	4	11.363	11.220	10.154	1.00	1.59	C
611	HETATM	28	HN1	NIT	4	11.813	10.440	10.389	1.00	1.89	H

tab:map

Table 3.1: Description of the XML mapping file (`map.xml`).

topology	Definitions of molecules, segments, and fragments.
molecules	Container for all molecules.
molecule	Mapping of a single molecule.
name	Name of the molecule in the coarse-grained model.
ident	Name (identification) of the molecule in the all-atom representation. This must match the molecule name in the atomistic representation.
segments	Partitioning of the molecule on conjugated segments.
segment	Description of a conjugated segment.
name	Name of a conjugated segment in a molecule.
fragments	Container for all fragments in a segment.
fragment	Description of a rigid fragment.
name	Name of the rigid fragment in a conjugated segment
mdatoms	List of all atoms belonging to the rigid fragment in the format residue number:residue name:atom name.
qmatoms	List of atoms of the rigid fragment in its ground state geometry, atom number:atom type.
weights	Weights are used to determine the fragment center. The order should be the same as in the mdatoms and qmatoms definitions. If the mass of a nucleus in atomic mass units is used, the center of the rigid fragment will be its center of mass.
localframe	Three atoms which define a local frame for each rigid fragment.

3.2 Mapping file

The mapping file (referred here as `map.xml`) is used by the program `xtp_map` to convert an atomistic trajectory to a trajectory with conjugated segments and rigid fragments. This trajectory is stored in a `state file` and contains positions, names, types of atoms belonging to rigid fragments. The description of the mapping options is given in table 3.1. An example of `map.xml` for a DCV2T molecule is shown in listing 3.2.

The file `map.xml` contains the whole electrostatic information about the molecules as well as the structural information. The `toolpdb2map` creates a `map.xml` from a `pdb` file and is a good starting point for further refinement.

Listing 3.2: Examble of `map.xml` for DCV2T. Each rigid fragment (coarse-grained bead) is defined by a list of atoms. Atom numbers, names, and residue names should correspond to those used in GROMACS topology (see the corresponding listing 3.1 of the `pdb` file).

```

622 <!-- this file is used to conver an atomistic trajectory to conjugated segments -->
623 <!-- molecules -->
624 <!-- molecule -->
625 <!-- name -->
626 <!-- mdname -->
627 <!-- segments -->
628 <!-- segment -->
629 <!-- name -->
630 <!-- qmcoords -->
631 <!-- qmcoords -->
632 <!-- IZINDO INPUT -->
633 <!-- basisset -->
634 <!-- orbitals -->
635 <!-- torbital_h -->
636 <!-- EMULTIPOLE INPUT -->
637 <!-- multipoles_n -->
638 <!-- multipoles_h -->
639 <!-- map2md -->
640 <!-- map2md -->
641 <!-- map2md -->
642 <!-- map2md -->
643 <!-- map2md -->
644 <!-- map2md -->
645 <!-- map2md -->
646 <!-- map2md -->
647 <!-- map2md -->
648 <!-- map2md -->

```

```

649 <U_cC_nN_h>0.0</U_cC_nN_h> <!-- Site energy -->
650 <U_nC_nN_h>0.1</U_nC_nN_h> <!-- Reorg. discharge -->
651 <U_cN_cC_h>0.1</U_cN_cC_h> <!-- Reorg. charge -->
652
653 <!-- MD QM MP Mapping -->
654 <fragments>
655 <fragment>
656 <name>NI1</name> <!-- name of the rigid fragment within the segment -->
657 <!-- list of atoms in the fragment resnum:resname:atomname -->
658 <mdatoms>1:NIT:N1 1:NIT:CN1 1:NIT:N2 1:NIT:CN2 1:NIT:CC1 1:NIT:C1 1:NIT:HN1</mdatoms>
659 <!-- corresponding ground state geometry atomnumber:atomtype read from .xyz file-->
660 <qmatoms> 20:N 19:C 14:N 13:C 12:C 11:C 23:H </qmatoms>
661 <!-- corresponding group state geometry multipoles read from .mps files -->
662 <mpoles> 20:N 19:C 14:N 13:C 12:C 11:C 23:H </mpoles>
663 <!-- weights to determine the fragment center (here CoM is used) -->
664 <weights> 14 12 14 12 12 12 1 </weights>
665 <!-- three atoms: define a cartesian local frame, two atoms: fragment is assumed to be
666 rotationally invariant around the axis, one atom: fragment is assumed isotropic -->
667 <localframe> 20 19 14 </localframe>
668 <!-- Optional parameters (if not set <localframe> is used): used when atom labels in the .mps
669 and .xyz file differ or more sites in the .mps file are used, so refers to <mpoles> -->
670 <localframe_mps> 20 19 14 </localframe_mps>
671 <!-- Optional parameters (if not set <localframe> is used): weights to determine the
672 fragment center (here CoM is used), used when atom labels in the .mps and .xyz file
673 differ or additional sites in the .mps file are used -->
674 <weights_mps> 14 12 14 12 12 12 1 </
675 weights_mps>
676 <!-- Optional flag: says if a site is virtual or not, (virtual=1, real=0)-->
677 <virtual_mps> 0 0 0 0 0 0 0 </
678 virtual_mps>
679 </fragment>
680
681 <fragment>
682 <name>TH1</name>
683 <mdatoms>2:THI:S1 2:THI:CA1 2:THI:CA2 2:THI:CB1 2:THI:CB2 2:THI:HC1 2:THI:HC2</mdatoms>
684 <qmatoms> 7:S 8:C 6:C 9:C 10:C 24:H 25:H </qmatoms>
685 <mpoles> 7:S 8:C 6:C 9:C 10:C 24:H 25:H </mpoles>
686 <weights> 32 12 12 12 12 1 1 </weights>
687 <localframe> 7 8 6 </localframe>
688 </fragment>
689
690 <fragment>
691 <name>TH2</name>
692 <mdatoms>3:THI:S1 3:THI:CA1 3:THI:CA2 3:THI:CB1 3:THI:CB2 3:THI:HC1 3:THI:HC2</mdatoms>
693 <qmatoms> 3:S 4:C 2:C 5:C 1:C 26:H 27:H </qmatoms>
694 <weights> 32 12 12 12 12 1 1 </weights>
695 <localframe> 3 4 2 </localframe>
696 </fragment>
697
698 <fragment>
699 <name>NI2</name>
700 <mdatoms>4:NIT:N1 4:NIT:CN1 4:NIT:N2 4:NIT:CN2 4:NIT:CC1 4:NIT:C1 4:NIT:HN1</mdatoms>
701 <qmatoms> 22:N 21:C 18:N 17:C 16:C 15:C 28:H </qmatoms>
702 <mpoles> 22:N 21:C 18:N 17:C 16:C 15:C 28:H </mpoles>
703 <weights> 14 12 14 12 12 12 1 </weights>
704 <localframe> 22 21 18 </localframe>
705 </fragment>
706 </fragments>
707 </segment>
708 </segments>
709 </molecule>
710 </molecules>
711 </topology>

```

3.3 Molecular orbitals

If the semi-empirical method is used to calculate electronic coupling elements, molecular orbitals of all molecules must be supplied. They can be generated using Gaussian program. The Gaussian input file for DCV2T is shown in listing 3.3. Provided with this input, Gaussian will generate *fort.7* file which contains the molecular orbitals of a DCV2T. This file can be renamed to *DCV2T.orb*. Note that the order of the atoms in the input file and the order of coefficients should always match. Therefore, the coordinate part of the input file must be supplied together with the orbitals. We will assume the coordinates, in the format *atom_type: x y z*, is saved to the *DCV2T.xyz* file.

Izindo requires the specification of orbitals for hole and electron transport in `map.xml`. They are the HOMO and LUMO respectively and can be retrieved from the `log` file from which the `DCV2T.orb` file is generated. The number of alpha electrons is the HOMO, the LUMO is HOMO+1

list:zindo_orbitals

Listing 3.3: Gaussian input file `get_orbitals.com` used for generating molecular orbitals. The first line contains the name of the check file, the second the requested RAM. `int=zindos` requests the method ZINDO, `punch=mo` states that the molecular orbitals ought to be written to the `fort.7` file, `nosymm` forbids use of symmetry and is necessary to ensure correct position of orbitals with respect to the provided coordinates. The two integer numbers correspond to the charge and multiplicity of the system: 0 1 corresponds to a neutral system with a multiplicity of one. They are followed by the types and coordinates of all atoms in the molecule.

```

724
725 %chk=DCV2T.chk
726 %mem=100Mb
727 #p int=zindos punch=mo nosymm
728
729 DCV2T molecular orbitals
730
731 0 1
732 S      -1.44650      2.12185      0.00135
733 C      -2.43098      0.58936     -0.00048
734 C      -1.59065     -0.51859     -0.00146
735 C      -0.21222     -0.22233     -0.00095
736 C       0.07761      1.13376      0.00040
737 S       2.87651      0.79316      0.00148
738 C       3.86099      2.32565      0.00235
739 C       3.02066      3.43359      0.00231
740 C       1.64223      3.13733      0.00162
741 C       1.35240      1.78125      0.00114
742 C      -3.85350      0.52245     -0.00081
743 C      -4.79569      1.52479     -0.00008
744 C      -6.18500      1.18622     -0.00117
745 C      -4.47544      2.91565      0.00081
746 C       5.28350      2.39256      0.00296
747 C       6.22569      1.39020      0.00327
748 C       7.61500      1.72876      0.00432
749 C       5.90542     -0.00064      0.00333
750 N      -7.32389      0.89743     -0.00195
751 N      -4.21872      4.06274      0.00142
752 N       8.75389      2.01754      0.00510
753 N       5.64864     -1.14772      0.00361
754 H      -1.98064     -1.52966     -0.00256
755 H       0.55785     -0.98374     -0.00169
756 H       3.41065      4.44466      0.00272
757 H       0.87216      3.89874      0.00147
758 H      -4.24640     -0.49192     -0.00188
759 H       5.67641      3.40692      0.00337
760

```

3.4 Monomer calculations for DFT transfer integrals

list:edft_gaussian_xml

Listing 3.4: Example `package.xml` file for the Gaussian package required in the options of the `edft calculator` for the monomer calculations as preparation for the determination of transfer integrals using DIPRO.

```

762
763 <package>
764   <name>gaussian</name>
765   <executable>g09</executable>
766   <checkpoint></checkpoint>
767   <scratch></scratch>
768
769   <charge>0</charge>
770   <spin>1</spin>
771   <options># pop=minimal pbepbe/6-311g** scf=tight punch=mo nosymm test</options>

```

```

772 <memory>1Gb</memory>
773 <threads>2</threads>
774
775 <cleanup></cleanup>
776 </package>

```

list:edft_turbomole.xml

Listing 3.5: Example package.xml file for the Turbomole package required in the options of the **edft calculator** for the monomer calculations as preparation for the determination of transfer integrals using DIPRO.

```

778 <package>
779 <name>turbomole</name>
780 <executable>ridft</executable>
781 <scratch>/tmp</scratch>
782
783 <options>
784 TITLE
785 a coord
786 *
787 no
788 b all def-TZVP
789 *
790 eht
791 y
792 0
793 y
794 dft
795 on
796 func
797 pbe
798 grid
799 m3
800 *
801 ri
802 on
803 m 300
804 *
805 scf
806 conv
807 7
808 iter
809 200
810
811 marij
812
813 q
814 </options>
815
816 <cleanup></cleanup>
817 </package>

```

list:edft_nwchem.xml

Listing 3.6: Example package.xml file for the NWChem package required in the options of the **edft calculator** for the monomer calculations as preparation for the determination of transfer integrals using DIPRO.

```

820 <package>
821 <name>nwchem</name>
822 <executable>nwchem</executable>
823 <checkpoint></checkpoint>
824 <scratch>/tmp/nwchem</scratch>
825 <charge>0</charge>
826 <spin>1</spin>
827 <threads>1</threads>
828 <memory></memory>
829 <options>
830 start

```

```

832 basis
833   * library 6-311gss
834 end
835 memory 1500 mb
836
837 dft
838   xc xpbe96 cpbe96
839   direct
840   iterations 100
841   noprint "final vectors analysis"
842 end
843 task dft
844 </options>
845   <cleanup></cleanup>
846 </package>

```

3.5 Pair calculations for DFT transfer integrals

list:ldft_gaussian.xml

Listing 3.7: Example package.xml file for the Gaussian package required in the options of the `ldft` calculator for the pair calculations and the determination of transfer integrals using DIPRO.

```

849
850 <package>
851   <name>gaussian</name>
852   <executable>g09</executable>
853   <checkpoint></checkpoint>
854   <scratch></scratch>
855
856   <charge>0</charge>
857   <spin>1</spin>
858   <options># pop=minimal pbepbe/6-311g** nosymm IOp(3/33=1,3/36=-1) punch=mo guess=cards scf=(maxcycle=1,
859   <memory>1Gb</memory>
860   <threads>1</threads>
861
862   <cleanup></cleanup>
863 </package>

```

list:ldft_turbomole.xml

Listing 3.8: Example package.xml file for the Turbomole package required in the options of the `ldft` calculator for the pair calculations and the determination of transfer integrals using DIPRO.

```

865
866 <package>
867   <name>turbomole</name>
868   <executable>ridft</executable>
869   <scratch>tmp</scratch>
870
871   <options>
872 $intsdebug cao
873 a coord
874 *
875 no
876 b all def-TZVP
877 *
878 eht
879 y
880 0
881 y
882 dft
883 on
884 func
885 pbe
886 grid
887 m3
888 *
889 ri
890 on

```

```

891 m 300
892 *
893 scf
894 conv
895 7
896 iter
897 1
898 diis
899 3
900 damp
901 0.00
902
903
904
905 marij
906
907 q
908 </options>
909
910 <cleanup></cleanup>
911 </package>

```

list:tdft_nwchem.xml

Listing 3.9: Example package.xml file for the NWChem package required in the options of the `tdft` calculator for the pair calculations and the determination of transfer integrals using DIPRO.

```

913
914 <package>
915   <name>nwchem</name>
916   <executable>nwchem</executable>
917   <checkpoint></checkpoint>
918   <scratch>tmp/nwchem</scratch>
919   <charge>0</charge>
920   <spin>1</spin>
921   <memory></memory>
922   <threads>1</threads>
923   <options>
924     start
925     basis
926     * library 6-311gss
927     end
928     memory 1500 mb
929
930     dft
931     print "ao overlap"
932     xc xpbe96 cpbe96
933     direct
934     iterations 1
935     convergence nodamping nodiis
936     noprint "final vectors analysis"
937     vectors input system.movecs
938     end
939     task dft
940   </options>
941   <cleanup></cleanup>
942 </package>
943

```

3.6 DFT transfer integrals

list:TI.xml

Listing 3.10: Example TI.xml file created as the output of a DIPRO calculation. Due to slightly different implementations, the orbitals indices refer to monomer indices in a Gaussian run but to indices in the merged dimer guess in a Turbomole run.

```

945
946 <pair name="pair_100_155">
947   <parameters>
948     <HOMO_A>162</HOMO_A>

```

```

949     <NoccA>1</NoccA>
950     <LUMO_A>164</LUMO_A>
951     <NvirtA>1</NvirtA>
952     <HOMO_B>161</HOMO_B>
953     <NoccB>1</NoccB>
954     <LUMO_B>163</LUMO_B>
955     <NvirtB>1</NvirtB>
956   </parameters>
957   <transport name="hole">
958     <channel name="single">
959       <J>1.546400416750696E-003</J>
960       <e_A>-6.30726450715697</e_A>
961       <e_B>-6.36775613794166</e_B>
962     </channel>
963     <channel name="multi">
964       <molecule name="A">
965         <e_HOMOm0>-6.30726450715697</e_HOMOm0>
966       </molecule>
967       <molecule name="B">
968         <e_HOMOm0>-6.36775613794166</e_HOMOm0>
969       </molecule>
970       <dimer name="integrals">
971         <T_00>1.546400416750696E-003</T_00>
972         <J_sq_degen>2.391354248926727E-006</J_sq_degen>
973         <J_sq_boltz>2.391354248926727E-006</J_sq_boltz>
974       </dimer>
975     </channel>
976   </transport>
977   <transport name="electron">
978     <channel name="single">
979       <J>-2.797473760331286E-003</J>
980       <e_A>-4.50318366770689</e_A>
981       <e_B>-4.53143397059021</e_B>
982     </channel>
983     <channel name="multi">
984       <molecule name="A">
985         <e_LUMOp0>-4.50318366770689</e_LUMOp0>
986       </molecule>
987       <molecule name="B">
988         <e_LUMOp0>-4.53143397059021</e_LUMOp0>
989       </molecule>
990       <dimer name="integrals">
991         <T_00>-2.797473760331286E-003</T_00>
992         <J_sq_degen>7.825859439742066E-006</J_sq_degen>
993         <J_sq_boltz>7.825859439742066E-006</J_sq_boltz>
994       </dimer>
995     </channel>
996   </transport>
997 </pair>
998

```

3.7 State file

999

sec:statefile

1000 All data structures are saved to the **state.sql** file in sqlite3 format, see <http://www.sqlite.org/>. They are
 1001 available in form of tables in the **state.sql** file as can be seen by the command
 1002 `sqlite3 state.sql " .tables "`

1003 An example of such a table are molecules. The full table can be displayed using the command (similar
 1004 for the other tables)

1005 `sqlite3 state.sql " SELECT * FROM molecules "`

1006 The meaning of all the entries in the table can be displayed by a command like

1007 `sqlite3 state.sql " .SCHEMA molecules "`

1008 The first and second entry are integers for internal and regular id of the molecule and the third entry is the
 1009 name. A single field from the table like the name of the molecule can be displayed by a command like

```

1010 sqlite3 state.sql " SELECT name FROM molecules "
1011 Besides molecules, the following tables are stored in the state.sql:
1012 conjseg_properties:
1013 Conjugated segments are stored with id, name and x,y,z coordinates of the center of mass in nm.
1014 conjsegs:
1015 Reorganization energies for charging or discharging a conjugated segment are stored together with the
1016 coulomb energy and any other user defined energy contribution (in eV) and occupation probabilities.
1017 pairs:
1018 The pairs from the neighborlist are stored with the pair id, the id of the first and second segment, the rate
1019 from the first to the second , the rate from the second to the first (both in  $s^{-1}$ ) and the x,y,z coordinates in
1020 nm of the distance between the first and the second segment.
1021 pairintegrals:
1022 Transfer integrals for all pairs are stored in the following way: The pair id , the number for counting
1023 possible different electronic overlaps (e.g if only the frontier orbitals are taken into account this is always
1024 zero, while an effective value is stored in addition to the different overlaps of e.g. HOMO-1 and HOMO-1
1025 if more frontier orbitals are taken into account) and the integral in eV.
1026 pairproperties:
1027 The outer sphere reorganization energy of all pairs is stored by an id, the pair id, a string lambda_outer
1028 and the energy in eV.
1029 conjsegs:
1030 Conjugated segments are saved in the following way: The id, the name, the type, the molecule id, the time
1031 frame, the x,y,z coordinates in nm and the occupation probability.
1032 conjseg_properties:
1033 Properties of the conjugated segments like reorganization energies for charging or discharging a charge
1034 unit or the coulomb contribution to the site energy are stored by: id, conjugated segment id, a string like
1035 lambda_intra_charging, lambda_intra_discharging or energy_coulomb and a corre-
1036 sponding value in eV.
1037 The tables rigidfrag_properties, rigidfrags and frames offer information about rigid frag-
1038 ments and time frames including periodic boundary conditions.
1039 The data in the state.sql file can also be modified by the user. Here is an example how to modify
1040 the transfer integral between the conjugated segments number one and two assuming that they are in the
1041 neighborlist. Their pair id can be found by the command
1042 pair_ID='sqlite3 state.sql "SELECT _id FROM pairs WHERE conjseg1=1 AND conjseg2=2" '
1043 The old value of the transfer integral can be deleted using
1044 sqlite3 state.sql "DELETE FROM pair_integrals WHERE pair=$pair_ID"
1045 Finally the new transfer integral J can be written to the state.sql file by the command
1046 sqlite3 state.sql "INSERT INTO pair_integrals (pair,num,J) VALUES ($pair_ID,0,$J)"
1047 Here the num=0 indicates that only the effective transfer integrals is written to the file, while other values
1048 of num would correspond to overlap between other orbitals than the frontier orbitals.
1049 In a similar way the coulomb contribution to the site energy of the first conjugated segment can be over-
1050 written by first getting its id
1051 c_ID='sqlite3 state.sql "SELECT _id from conjseg_properties where conjseg=1 AND
1052 key =\"energy_coulomb\" "
1053 Then deleting the old value
1054 sqlite3 state.sql "DELETE FROM conjseg_properties WHERE _id=$c_ID"
1055 Then the new coulomb energy E can be written to this id
1056 sqlite3 state.sql "INSERT INTO conjseg_properties (_id,conjseg,key,value)
1057 VALUES ($c_ID,1,\"energy_coulomb\",$E)"
1058 Finally the resulting coulomb contribution to all conjugated segments can be displayed by
1059 sqlite3 state.sql "SELECT * from conjseg_properties WHERE key=\"energy_coulomb\" "
1060

```

1061

Chapter 4

1062

Reference

sec:reference

1063

4.1 Programs

sec:programs

1064

Programs execute specific tasks (calculators).

1065

4.1.1 xtp_testsuite

prog:xtp_testsuite

1066

Performs tests en suite + optional arguments:

1067

-h, --help show this help message and exit

1068

-e [[...]], --execute [[...]] Tests to perform, accepts regex (def=".)*

1069

-l, --listonly List all tests available, then quit.

1070

-x, --xml Test-suite file (def="\$VOTCASHARE/xtp/xml/testsuite.xml")

1071

-s, --source Test source input directory (def="source")

1072

-td, --testdirectory Test run directory (def="suite")

1073

-t, --target Directory where to store targets (def="targets")

1074

-r, --reference Folder with reference data to compare to (def="reference")

1075

-g, --generate Generate reference from targets (def=False)

1076

-cmp, --compareonly Only compare existing targets to reference (def=False)

1077

-v, --verbose The wordy version (def=False)

1078

-sh, --showoutput Display VOTCA::XTP exec. output (def=False)

1079

-c, --clean To clean or not to clean test dir. (def=False)

1080

-m, --mailto Mail the result. (def=False)

1081

4.1.2 xtp_update

prog:xtp_update

1082

Updates the state file + optional arguments:

1083

-h, --help show this help message and exit

1084

-f SQLFILE, --file SQLFILE State file to update.

1085

4.1.3 xtp_update_exciton

prog:xtp_update_exciton

1086

Updates the state file for singlets and triplets + optional arguments:

1087

-h, --help show this help message and exit

1088

-f SQLFILE, --file SQLFILE State file to update.

1089

4.1.4 xtp_basisset

prog:xtp_basisset

1090

xtp_update, version 1.4-dev gitid: 0c0a762 Creates votca xml basissetfiles from NWCHEM basissetfiles

1091

optional arguments:

```

1092     -h, --help show this help message and exit
1093     -f NWCHEM, --inputnw NWCHEM NWchem file containing the basisset.
1094     -o OUTPUTFILE, --outputvotca OUTPUTFILE Path of votca outputfile

```

4.1.5 xtp_map

prog:xtp_map

```

1096 Generates QM|MD topology
1097     -h [ --help ] display this help and exit
1098     -v [ --verbose ] be loud and noisy
1099     -t [ --topology ] arg topology
1100     -c [ --coordinates ] arg coordinates or trajectory
1101     -s [ --segments ] arg definition of segments and fragments
1102     -f [ --file ] arg state file

```

4.1.6 xtp_run

prog:xtp_run

```

1104 Runs excitation/charge transport calculators
1105     -h [ --help ] display this help and exit
1106     -v [ --verbose ] be loud and noisy
1107     -o [ --options ] arg calculator options
1108     -f [ --file ] arg sqlight state file, *.sql
1109     -i [ --first-frame ] arg (=1) start from this frame
1110     -n [ --nframes ] arg (=1) number of frames to process
1111     -t [ --nthreads ] arg (=1) number of threads to create
1112     -s [ --save ] arg (=1) whether or not to save changes to state file
1113     -e [ --execute ] arg List of calculators separated by ',' or ''
1114     -l [ --list ] Lists all available calculators -d [ --description ] arg Short description of a cal-
1115         culator

```

4.1.7 xtp_tools

prog:xtp_tools

```

1117 Runs excitation/charge transport tools
1118     -h [ --help ] display this help and exit
1119     -v [ --verbose ] be loud and noisy
1120     -t [ --nthreads ] arg (=1) number of threads to create
1121     -o [ --options ] arg calculator options Tools:
1122     -e [ --execute ] arg List of tools separated by ',' or ''
1123     -l [ --list ] Lists all available tools -d [ --description ] arg Short description of a tool

```

4.1.8 xtp_parallel

prog:xtp_parallel

```

1125 Runs job-based heavy-duty calculators
1126     -h [ --help ] display this help and exit
1127     -v [ --verbose ] be loud and noisy
1128     -o [ --options ] arg calculator options
1129     -f [ --file ] arg sqlite state file, *.sql
1130     -i [ --first-frame ] arg (=1) start from this frame
1131     -n [ --nframes ] arg (=1) number of frames to process
1132     -t [ --nthreads ] arg (=1) number of threads to create
1133     -s [ --save ] arg (=1) whether or not to save changes to state file
1134     -r [ --restart ] arg restart pattern: 'host(pc1:234) stat(FAILED)'
1135     -c [ --cache ] arg (=8) assigns jobs in blocks of this size
1136     -j [ --jobs ] arg (=run) task(s) to perform: input, run, import

```



```

1137 -m [ --maxjobs ] arg (=1) maximum number of jobs to process (-1 = inf)
1138 -e [ --execute ] arg List of calculators separated by ',' or ''
1139 -l [ --list ] Lists all available calculators -d [ --description ] arg Short description of a cal-
1140 culator

```

1141 4.1.9 xtp_dump

prog:xtp_dump

```

1142 Extracts information from the state file
1143 -h [ --help ] display this help and exit
1144 -v [ --verbose ] be loud and noisy
1145 -o [ --options ] arg calculator options
1146 -f [ --file ] arg sqlight state file, *.sql
1147 -i [ --first-frame ] arg (=1) start from this frame
1148 -n [ --nframes ] arg (=1) number of frames to process
1149 -t [ --nthreads ] arg (=1) number of threads to create
1150 -s [ --save ] arg (=1) whether or not to save changes to state file Extractors:
1151 -e [ --extract ] arg List of extractors separated by ',' or ''
1152 -l [ --list ] Lists all available extractors -d [ --description ] arg Short description of an ex-
1153 tractor

```

1154 4.1.10 xtp_overlap

prog:xtp_overlap

```

1155 moo_overlap
1156 -h [ --help ] display this help and exit
1157 -v [ --verbose ] be loud and noisy MOO Options:
1158 --conjseg arg xml file describing two conjugated segments
1159 --pos1 arg position and orientation of molecule 1
1160 --pos2 arg position and orientation of molecule 2
1161 --pdb arg (=geometry.pdb) pdb file of two molecules

```

1162 4.1.11 xtp_kmc_run

prog:xtp_kmc_run

```

1163 kmc_run, version 1.4-dev gitid: 0c0a762 (compiled Sep 15 2016, 05:12:17) Runs specified calculators
1164 -h [ --help ] display this help and exit
1165 -v [ --verbose ] be loud and noisy
1166 -o [ --options ] arg program and calculator options
1167 -f [ --file ] arg sqlite state file
1168 -t [ --textfile ] arg output text file (otherwise: screen output)
1169 -e [ --execute ] arg list of calculators separated by commas or spaces
1170 -l [ --list ] lists all available calculators -d [ --description ] arg detailed description of a
1171 calculator

```

1172 4.2 Calculators

sed:calculators

```

1173 Calculator is a piece of code which computes specific system properties, such as site energies, transfer
1174 integrals, etc. xtp_run, xtp_kmc_run are wrapper programs which executes such calculators. The
1175 generic syntax is
1176 xtp_run -e "calc1, calc2, ..." -o options.xml
1177 File options.xml lists all options needed to run a specific calculator. The format of this file is explained
1178 in listing 4.1. A complete list of calculators is given in the calculators reference section.

```

list:calc

Listing 4.1: A part of the options.xml file with options for the calculator_name{1,2} calculators.

```

1179
1180 <calculator_name1>
1181     <option1>value1</option1>
1182     <option2>value2</option2>
1183     ...
1184 </calculator_name1>
1185
1186 <calculator_name2>
1187     <option1>value1</option1>
1188     <option2>value2</option2>
1189     ...
1190 </calculator_name2>
1191 ...

```

1193 A list of all calculators and their short descriptions can be obtain using

1194 `xtp_run --list`

1195 A detailed description of all options of a specific calculator(s) is available via

1196 `xtp_run --desc calc1,calc2,...`

1197 4.2.1 coupling

calc:coupling

1198 Electronic couplings from log and orbital files (GAUSSAIN, TURBOMOLE, NWChem)

option	default	unit	description
package			First-principles package
output	coupling.out.xml		Output file
degeneracy	0	eV	Criterion for the degeneracy of two levels
moleculeA			
log	A.log		Log file of molecule A
orbitals	A.orb		Orbitals file
levels	3		Output HOMO, ..., HOMO-levels; LUMO, ..., LUMO+levels
trim	2		
moleculeB			
log	B.log		Log file of molecule B
orbitals	B.orb		Orbitals file
levels	3		Output HOMO, ..., HOMO-levels; LUMO, ..., LUMO+levels
trim	2		
dimerAB			
log	AB.log		Log file of dimer AB
orbitals	A.orb		Orbitals file

1199 Return to the description of `coupling`.

1200 4.2.2 excitoncoupling

calc:excitoncoupling

1201 Exciton couplings from serialized orbital files

option	default	unit	description
output	excitoncoupling.c		Output file
bsecoupling			
orbitalsA	A.orb		Serialized orbitals file
orbitalsB	B.orb		Serialized orbitals file
orbitalsAB	AB.orb		Serialized orbitals file

1202 Return to the description of `excitoncoupling`.

4.2.3 gencube

1203
calc:gencube
1204

Tool to generate cube files from .orb file

option	default	unit	description
output	state.cube		Output file
input	system.orb		Input file
padding	6.5		How far the grid should start from the molecule
xsteps	25		Gridpoints in x-direction
ysteps	25		Gridpoints in y-direction
zsteps	25		Gridpoints in z-direction
state	1		State to generate cube file for
spin			Singlet or Triplet
type	ground		qp:quasiparticle,ground:groundstate,transition:transitionstate,excited/excited-gs:excitedstate density/density excited-ground state
mode	new		new: generate new cube file, subtract: subtract to cube files specified below
infile1			Cubefile to subtract infile2 from
infile2			Cubefile to subtract from infile1

1205 Return to the description of [gencube](#).

4.2.4 log2mps

1206
calc:log2mps
1207

Generates an mps-file (with polar-site definitions) from a QM log-file

option	default	unit	description
package			QM package
logfile			Log-file generated by QM package, with population/esp-fit data

1208 Return to the description of [log2mps](#).

4.2.5 molpol

1209
calc:molpol
1210

Molecular polarizability calculator (and optimizer)

option	default	unit	description
mpsfiles			
input			mps input file
output			mps output file
polar			xml file with infos on polarizability tensor
induction			
expdamp			Thole sharpness parameter
wSOR			mixing factor for convergence
maxiter			maximum number of iterations
tolerance			rel. tolerance for induced moments
target			
optimize			if 'true', refine atomic polarizabilities to match molecular polarizable volume specified in target.molpol
molpol			target polarizability tensor in format xx xy xz yy yz zz (this should be in the eigen-frame, hence xy = xz = yz = 0), if optimize=true the associated polarizable volume will be matched iteratively and the resulting set of polar sites written to mps-files.output
tolerance			relative tolerance when optimizing the polarizable volume

1211 Return to the description of [molpol](#).

4.2.6 orb2isogwa

1212
calc:orb2isogwa
1213

Analysis tool for QM results stores in serialized file

option	default	unit	description
output	qmanalyze.out		Output file
property			
input	molecule.orb		Serialized file

1214 Return to the description of [orb2isogwa](#).

4.2.7 partialcharges

1215
calc:partialcharges
1216

Tool to derive partial charges from QM results stores in serialized file

option	default	unit	description
output	Moleculecharges.		Output file either .mps or .pdb
input	molecule.orb		Serialized file
esp2multipole			options for the method

1217 Return to the description of [partialcharges](#).

4.2.8 pdb2map

1218
calc:pdb2map
1219

Converts MD + QM files to VOTCA mapping. Combinations: *pdb+xyz,gro+xyz,pdb*

option	default	unit	description
pdb	conf.pdb		Input pdb file
gro	conf.gro		Input gro file
xyz	conf.xyz		Input xyz file
xml	conf.xml		Resulting xml file

1220 Return to the description of [pdb2map](#).

4.2.9 pdb2top

1221
calc:pdb2top
1222

Generates fake Gromacs topology file .top

option	default	unit	description
num	1		Num of mols in the box
pdb	conf.pdb		Input pdb file
gro	conf.gro		Input gro file

1223 Return to the description of [pdb2top](#).

4.2.10 ptopreader

1224
calc:ptopreader
1225

Reads binary .ptop-files (serialized from ewdbgp) and processes them into something readable

option	default	unit	description
ptop_file			Binary archive .ptop-file

1226 Return to the description of [ptopreader](#).

4.2.11 qmanalyze

1227

calc:qmanalyze

1228

Analysis tool for QM results stores in serialized file

option	default	unit	description
output	qmanalyze.out		Output file
BSE			additonal info about BSE results
input	molecule.orb		Serialized file

1229 Return to the description of [qmanalyze](#).

4.2.12 eanalyze

1230

calc:eanalyze

1231

Histogram and correlation function of site energies and pair energy differences

option	default	unit	description
resolution_sites		eV	Bin size for site energy histogram
resolution_pairs		eV	Bin size for pair energy histogram
resolution_space		eV	Bin size for site energy correlation
states			?

1232 Return to the description of [eanalyze](#).

4.2.13 eimport

1233

calc:eimport

1234

Imports site energies from the output file of emultipole and writes them to the state file

option	default	unit	description
--------	---------	------	-------------

1235 Return to the description of [eimport](#).

4.2.14 einternal

1236

calc:einternal

1237

Reads in site and reorganosation energies and writes them to the state file

option	default	unit	description
energiesXML			XML input file with vacuum site, reorganization (charging, discharging) energies

1238 Return to the description of [einternal](#).

4.2.15 emultipole

1239

calc:emultipole

1240

Evaluates polarization contribution based on the Thole model

option	default	unit	description
multipoles			Polar Site Definitions in GDMA punch-file format
control			Control options for induction computation
induce	1		Enter '1' / '0' to toggle induction on / off
first			First segment for which to compute site energies
last			Last segment for which to compute site energies
output			File to write site energies to. Site energies are also stored in the state file
check			Check mapping of polar sites to fragment
tholeparam			Thole parameters required for charge-smearing
cutoff		nm	Cut-off beyond which all interactions are neglected

cutoff2		nm	Cut-off beyond which polarization is neglected
expdamp			Damping exponent used in exponential damping function
scaling			1-n interaction scaling, currently not in use
esp			Control options for potential calculation
calcESP			Enter '1' / '0' to toggle on / off. If '1', site energies will not be evaluated
cube			
grid			XYZ file specifying grid points for potential evaluation
output			File to write grid-point potential to
esf			Control options for field calculation
calcESF			Enter '1' / '0' to toggle on / off. If '1', site energies will not be evaluated
grid			XYZ file specifying grid points for field evaluation
output			File to write grid-point field to
alphamol			Control options for molecular-polarizability calculation
calcAlpha			Enter '1' / '0' to toggle on / off. If '1', site energies will not be evaluated
output			File to write polarizability tensor in global frame and in diagonal form to
convparam			Convergence parameters for self-consistent field calculation
wSOR_N			Mixing factor for successive overrelaxation of neutral system, usually between 0.3 and 0.5
wSOR_C			Mixing factor for successive overrelaxation of charged system, usually between 0.3 and 0.5
tolerance			Convergence criterion, fulfilled if relative change smaller than tolerance
maxiter			Maximum number of iterations in the convergence loop

1241 Return to the description of [emultipole](#).

1242 4.2.16 eoutersphere

calc:eoutersphere

1243 Evaluates outersphere reorganization energy

option	default	unit	description
multipoles			XML allocation polar sites
method			Type of the method: constant - all pairs have value lambda . spheres - molecules are treated as spheres with radii radius and Pekar factor pekar . dielectric - with Pekar factor pekar and partial charges from resulting dielectric fields
lambdaconst		eV	The value for all pairs in the constant method
pekar			Pekar factor used for methods spheres and dielectric
segment			
type			
radius			
segment			
type			
radius			
cutoff		nm	Cutoff radius in between pair and the exterior molecule. Can be used in spheres and dielectric

1244 Return to the description of [eoutersphere](#).

1245 4.2.17 ianalyze

calc:ianalyze

1246 Evaluates a histogram of a logarithm of squared couplings

option	default	unit	description
resolution_logJ2			Bin size of histogram $\log(J2)$
resolution_space		nm	Bin size for r in $\log(J2(r))$
states			States for which to calculate the histogram. Example: 1 -1

1247 Return to the description of [ianalyze](#).

1248 4.2.18 iimport

calc:iimport

1249 Imports electronic couplings from xml of xtp-dipro using folders of pairedump

option	default	unit	description
idft_jobs_file			idft jobs file
probabilityfile_h	ianalyze.ispatial-h.out		For coarse grained simulations provide here the distance dependent means and sigmas of hole transfer integrals. This file can be created using the ianalyze calculator.
probabilityfile_e	ianalyze.ispatial-e.out		For coarse grained simulations provide here the distance dependent means and sigmas of electron transfer integrals. This file can be created using the ianalyze calculator.

1250 Return to the description of [iimport](#).

1251 4.2.19 izindo

calc:izindo

1252 Semiempirical electronic coupling elements for all neighbor list pairs

option	default	unit	description
orbitalsXML			File with paths to .orb files

1253 Return to the description of [izindo](#).

1254 4.2.20 jobwriter

calc:jobwriter

1255 Writes list of jobs for a parallel execution

option	default	unit	description
keys			job type
single_id			Segment ID as argument for mps.single
kmc_cutoff		nm	Pair-interaction cut-off as argument for mps.kmc

1256 Return to the description of [jobwriter](#).

1257 4.2.21 pairedump

calc:pairedump

1258 Coordinates of molecules and pairs from the neighbor list

option	default	unit	description
molecules			If true outputs single molecules, otherwise only pairs

1259 Return to the description of [pairedump](#).

1260 4.2.22 panalyze

calc:panalyze

1261 Probability of neighbours being in the pair list as a function of their centre of mass distance

option	default	unit	description
resolution_space		nm	Spatial resolution for the probability function.

1262 Return to the description of [panalyze](#).

1263 4.2.23 profile

calc:profile

1264 Density and site energy profiles

option	default	unit	description
axis			Axis along which to calculate density and energy profiles
direction	0 0 1		Axis direction
min		nm	Minimal projected position for manual binning
max		nm	Maximal projected position for manual binning
bin	0.1	nm	Spatial resolution of the profile
auto	1		'0' for manual binning using min and max, '1' for automated
particles			
type	segments		What centers of mass to use: 'segments' or 'atoms'
first	1		ID of the first segment
last	-1		ID of the last segment, -1 is the list end
output			
density	density.dat		Density profile file
energy	energy.dat		Energy profile file

1265 Return to the description of [profile](#).

1266 4.2.24 rates

calc:rates

1267 Hopping rates using classical or semi-classical expression

option	default	unit	description
field			Field in x y z direction
temperature		K	Temperature for rates
method			Method chosen to compute rates. Can either be marcus or jortner . The first is the high temperature limit of Marcus theory, the second is the rate proposed by Jortner and Bixon
nmaxvib	20		If the method of choice is jortner , the maximal number of excited vibrations on the molecules has to be specified as an integer for the summation
omegavib	0.2	eV	If the method of choice is jortner , the vibration frequency of the quantum mode has to be given in units of eV. The default value is close to the CC bond-stretch at 0.2eV

1268 Return to the description of [rates](#).

1269 4.2.25 sandbox

calc:sandbox

1270 Sandbox to test xtp classes

option	default	unit	description
ID			Not in use

1271 Return to the description of [sandbox](#).

4.2.26 stateserver

1272

calc:stateserver

1273

Export SQLite file to human readable format

option	default	unit	description
out			Output file name
pdb			PDB coordinate file name
keys			Sections to write to readable format (topology, segments, pairs, coordinates)

1274 *Return to the description of [stateserver](#).***4.2.27 tdump**

1275

calc:tdump

1276

Coarse-grained and back-mapped (using rigid fragments) trajectories

option	default	unit	description
md	MD.pdb		Name of the coarse-grained trajectory
qm	QM.pdb		Name of the trajectory with back-substituted rigid fragments
frames	1		Number of frames to output

1277 *Return to the description of [tdump](#).***4.2.28 vaverage**

1278

calc:vaverage

1279

Computes site-centered velocity averages from site occupancies

option	default	unit	description
carriers			Carrier types for which to compute velocity averages
tabulate			Tabulate 'atoms' or 'segments'

1280 *Return to the description of [vaverage](#).***4.2.29 zmultipole**

1281

calc:zmultipole

1282

Evaluates polarization contribution based on the Thole model

option	default	unit	description
multipoles			Polar Site Definitions in GDMA punch-file format
control			Control options for induction computation
induce	1		Enter '1' / '0' to toggle induction on / off
first			First segment for which to compute site energies
last			Last segment for which to compute site energies
output			File to write site energies to. Site energies are also stored in the state file
check			Check mapping of polar sites to fragment
tholeparam			Thole parameters required for charge-smearing
cutoff		nm	Cut-off beyond which all interactions are neglected
cutoff2		nm	Cut-off beyond which polarization is neglected
expdamp			Damping exponent used in exponential damping function
scaling			1-n interaction scaling, currently not in use
esp			Control options for potential calculation
calcESP			Enter '1' / '0' to toggle on / off. If '1', site energies will not be evaluated
cube			
grid			XYZ file specifying grid points for potential evaluation
output			File to write grid-point potential to

<i>esf</i>			Control options for field calculation
<i>calcESF</i>			Enter '1' / '0' to toggle on / off. If '1', site energies will not be evaluated
<i>grid</i>			XYZ file specifying grid points for field evaluation
<i>output</i>			File to write grid-point field to
<i>alphamol</i>			Control options for molecular-polarizability calculation
<i>calcAlpha</i>			Enter '1' / '0' to toggle on / off. If '1', site energies will not be evaluated
<i>output</i>			File to write polarizability tensor in global frame and in diagonal form to
<i>convparam</i>			Convergence parameters for self-consistent field calculation
<i>wSOR_N</i>			Mixing factor for successive overrelaxation of neutral system, usually between 0.3 and 0.5
<i>wSOR_C</i>			Mixing factor for successive overrelaxation of charged system, usually between 0.3 and 0.5
<i>tolerance</i>			Convergence criterion, fulfilled if relative change smaller than tolerance
<i>maxiter</i>			Maximum number of iterations in the convergence loop

1283 Return to the description of *zmultipole*.

1284 4.2.30 edft

calc:edft

1285 A wrapper for first principles based single site calculations

option	default	unit	description
<i>job</i>			Job options
<i>tasks</i>	<i>input,run,parse</i>		What to run
<i>store</i>	<i>orbitals</i>		What to store

1286 Return to the description of *edft*.

1287 4.2.31 egwbse

calc:egwbse

1288 An implementation of GW-BSE.

option	default	unit	description
<i>job</i>			Job options
<i>dftbasis</i>			
<i>gwbasis</i>			
<i>rpamax</i>			
<i>qpmin</i>			
<i>qpmax</i>			
<i>bsemin</i>			
<i>bsemax</i>			
<i>shift</i>			
<i>tasks</i>			
<i>store</i>			
<i>exttotal</i>			
<i>print</i>			

1289 Return to the description of *egwbse*.

1290 4.2.32 idft

calc:idft

1291 Projection method for electronic couplings. Requires *edft* output

option	default	unit	description
tasks	input,run,parse,t		What to do
store	orbitals,overlap,in		What to store
degeneracy	0	eV	Criterion for the degeneracy of two levels
levels	3		Output between HOMO, ..., HOMO-levels; LUMO, ..., LUMO+levels
trim	2		Use trim*occupied of virtual orbitals

1292 Return to the description of [idft](#).

1293 4.2.33 igwbse

calc:igwbse

1294 Projection method for excitonic couplings. Requires gwbse output

option	default	unit	description
package			
job			
file			
tasks			
gwbse			
dftbasis			
gwbasis			
shift			
tasks			
exctotal			
print			
type	singlets		Spin types for couplings
degeneracy	0	eV	Criterion for the degeneracy of two levels
states	5		Number of excitons considered

1295 Return to the description of [igwbse](#).

1296 4.2.34 qmmm

calc:qmmm

1297 QM/MM with the Thole MM model

option	default	unit	description
control			
pdb_check			PDB file of polar sites
write_chk	dipoles.xyz		XYZ file with dipoles split onto point charges
format_chk	xyz		format, gaussian or xyz
split_dpl	1		'0' do not split dipoles onto point charges, '1' do split
dpl_spacing	1e-3	nm	Spacing to be used when splitting dipole onto point charges: $d = q * a$
qmpackage			
package			QM package to use for the QM region
gwbse			Specify if GW/BSE excited state calculation ist needed
gwbse_options			GW/BSE options file
state			Number of excited state, which is to be calculated
type			Character of the excited state to be calculated
filter			Filter with which to find the excited state after each calculation
oscilla-			Oscillator strength filter, only states with higher oscillator
tor_strength			strength are considered
charge_transfer			Charge transfer filter , only states with charge transfer above threshold are considered
qmmmconv			convergence criteria for the QM/MM
dR	0.001	nm	RMS of coordinates

<i>dQ</i>	0.001	<i>e</i>	RMS of charges
<i>dE_QM</i>	0.0001	<i>eV</i>	Energy change of the QM region
<i>dE_MM</i>	0.0001	<i>eV</i>	Energy change of the MM region
<i>max_iter</i>	10		Number of iterations
<i>coulombmethod</i>			Options for the MM embedding
<i>method</i>	<i>cut-off</i>		Method for evaluation of electrostatics
<i>cutoff1</i>			Cut-off for the polarizable MM1 shell
<i>cutoff2</i>			Cut-off for the static MM2 shell
<i>tholemodel</i>			Parameters for the Thole model
<i>induce</i>			'1' - induce '0' - no induction
<i>induce_intra_pair</i>			'1' - include mutual interaction of induced dipoles in the QM region. '0' - do not
<i>exp_damp</i>	0.39		Sharpness parameter
<i>scaling</i>			Bond scaling factors
<i>convergence</i>			Convergence parameters for the MM1 (polarizable) region
<i>wSOR_N</i>			Mixing factor for the successive overrelaxation algorithm for a neutral QM region
<i>wSOR_C</i>			Mixing factor for the successive overrelaxation algorithm for a charged QM region
<i>max_iter</i>	512		Maximal number of iterations to converge induced dipoles
<i>tolerance</i>			Maximum RMS change allowed in induced dipoles

1298 [Return to the description of `qmmm`.](#)

1299 4.2.35 `xqmultipole`

calc:xqmultipole

1300 Electrostatic interaction and induction energy of charged molecular clusters

<i>option</i>	<i>default</i>	<i>unit</i>	<i>description</i>
<i>multipoles</i>			Polar-site mapping definition
<i>control</i>			
<i>job_file</i>			Job file
<i>emp_file</i>			Polar-background definition, allocation of mps-files to segments
<i>pdb_check</i>			Whether or not to output a pdb-file of the mapped polar sites
<i>format_chk</i>			Format for check-file: 'xyz' or 'gaussian'
<i>split_dpl</i>			Split dipoles onto point charges in check-file
<i>dpl_spacing</i>		nm	Spacing between point charges for check-file output
<i>coulombmethod</i>			
<i>method</i>			Currently only cut-off supported
<i>cutoff1</i>		nm	Full-interaction radius cut-off
<i>cutoff2</i>		nm	Radius of electrostatic buffer
<i>tholemodel</i>			
<i>induce</i>			Induce - or not
<i>induce_intra_pair</i>			Induce mutually within the charged cluster
<i>exp_damp</i>			Thole sharpness parameter
<i>scaling</i>			Bond scaling parameters, currently not used
<i>convergence</i>			
<i>wSOR_N</i>			SOR mixing factor for overall neutral clusters
<i>wSOR_C</i>			SOR mixing factor for overall charged clusters
<i>max_iter</i>			Maximum number of iterations
<i>tolerance</i>			Relative tolerance as convergence criterion

1301 [Return to the description of `xqmultipole`.](#)

1302 4.2.36 `energy2xml`

calc:energy2xml

1303 Write out energies from SQL file

option	default	unit	description
--------	---------	------	-------------

1304 Return to the description of [energy2xml](#).

1305 4.2.37 integrals2xml

calc:integrals2xml

1306 Write out transfer integrals from SQL file

option	default	unit	description
--------	---------	------	-------------

1307 Return to the description of [integrals2xml](#).

1308 4.2.38 occupations2xml

calc:occupations2xml

1309 Write out site occupation probabilities from SQL file

option	default	unit	description
--------	---------	------	-------------

1310 Return to the description of [occupations2xml](#).

1311 4.2.39 pairs2xml

calc:pairs2xml

1312 Write out neighbourlist from SQL file

option	default	unit	description
--------	---------	------	-------------

1313 Return to the description of [pairs2xml](#).

1314 4.2.40 rates2xml

calc:rates2xml

1315 Write out charge transfer rates from SQL file

option	default	unit	description
--------	---------	------	-------------

1316 Return to the description of [rates2xml](#).

1317 4.2.41 segments2xml

calc:segments2xml

1318 Write out segment data from SQL file

option	default	unit	description
--------	---------	------	-------------

1319 Return to the description of [segments2xml](#).

1320 4.2.42 trajectory2pdb

calc:trajectory2pdb

1321 Generate PDB files for the mapped MD/QM topology

option	default	unit	description
--------	---------	------	-------------

1322 Return to the description of [trajectory2pdb](#).

1323

4.3 Common options

ref:options

<i>name</i>	<i>Description of the option</i>
-------------	----------------------------------

Bibliography

- [ruhle_microscopic_2011](#) [1] V. Rühle *et al.*, *J. Chem. Theory Comput.* **7**, 3335 (2011). [ii](#), [3](#), [17](#), [18](#)
- [ruhle_versatile_2009](#) [2] V. Rühle *et al.*, *J. Chem. Theory Comput.* **5**, 3211 (2009). [ii](#), [3](#), [6](#)
- [gamma_design_1995](#) [3] E. Gamma, R. Helm, and R. E. Johnson, Design Patterns. Elements of Reusable Object-Oriented Software., 1st ed., reprint. ed. (Addison-Wesley Longman, Amsterdam, ADDRESS, 1995). [3](#)
- [ruhle_multiscale_2010](#) [4] V. Rühle, J. Kirkpatrick, and D. Andrienko, *J. Chem. Phys.* **132**, 134103 (2010). [7](#)
- [vukmirovic_charge_2008](#) [5] N. Vukmirović and L.-W. Wang, *J. Chem. Phys.* **128**, 121102 (2008). [7](#)
- [vukmirovic_charge_2009](#) [6] N. Vukmirović and L.-W. Wang, *Nano Letters* **9**, 3996 (2009).
- [mcmahon_ad_2009](#) [7] D. P. McMahon and A. Troisi, *Chem. Phys. Lett.* **480**, 210 (2009). [7](#)
- [bredas_charge-transfer_2004](#) [8] J.-L. Brédas, D. Beljonne, V. Coropceanu, and J. Cornil, *Chem. Rev.* **104**, 4971 (2004). [8](#), [17](#)
- [breneman_determining_1990](#) [9] C. M. Breneman and K. B. Wiberg, *J. Comput. Chem.* **11**, 361–373 (1990). [10](#)
- [stone_distributed_1985](#) [10] A. Stone and M. Alderton, *Molecular Physics* **56**, 1047 (1985). [10](#), [11](#)
- [chirlian_atomic_1987](#) [11] L. E. Chirlian and M. M. Francl, *J. Comput. Chem.* **8**, 894 (1987). [10](#)
- [singh_approach_1984](#) [12] U. C. Singh and P. A. Kollman, *J. Comput. Chem.* **5**, 129 (1984). [11](#)
- [stone_distributed_2005](#) [13] A. J. Stone, *J. Chem. Theory Comput.* **1**, 1128 (2005). [11](#)
- [stone_theory_1997](#) [14] A. J. Stone, The Theory of intermolecular forces (Clarendon Press, Oxford, 1997). [11](#)
- [thole_molecular_1981](#) [15] B. Thole, *Chem. Phys.* **59**, 341 (1981). [12](#)
- [ren_polarizable_2003](#) [16] P. Ren and J. W. Ponder, *J. Phys. Chem. B* **107**, 5933 (2003). [12](#), [13](#)
- [troisi_charge-transport_2006](#) [17] A. Troisi and G. Orlandi, *Phys. Rev. Lett.* **96**, (2006). [13](#)
- [troisi_charge_2009](#) [18] A. Troisi, D. L. Cheung, and D. Andrienko, *Phys. Rev. Lett.* **102**, 116602 (2009).
- [mcmahon_organic_2010](#) [19] D. P. McMahon and A. Troisi, *ChemPhysChem* **11**, 2067 (2010). [13](#)
- [baumeier_density-functional_2010](#) [20] B. Baumeier, J. Kirkpatrick, and D. Andrienko, *Phys. Chem. Chem. Phys.* **12**, 11103 (2010). [13](#), [16](#), [17](#)
- [kirkpatrick_approximate_2008](#) [21] J. Kirkpatrick, *Int. J. Quantum Chem.* **108**, 51 (2008). [17](#)
- [walker_electrical_2002](#) [22] A. B. Walker, A. Kambili, and S. J. Martin, *J. Phys-Condens. Mat.* **14**, 9825 (2002). [17](#)
- [baessler_charge_1993](#) [23] H. Baessler, *Phys. Status Solidi B* **175**, 15 (1993).
- [borsenberger_charge_1991](#) [24] P. M. Borsenberger, L. Pautmeier, and H. Bässler, *J. Chem. Phys.* **94**, 5447 (1991).
- [pasveer_unified_2005](#) [25] W. F. Pasveer *et al.*, *Phys. Rev. Lett.* **94**, 206601 (2005). [17](#)
- [bredas_molecular_2009](#) [26] J.-L. Brédas, J. E. Norton, J. Cornil, and V. Coropceanu, *Accounts Chem. Res.* **42**, 1691 (2009). [17](#)
- [coropceanu_charge_2007](#) [27] V. Coropceanu *et al.*, *Chem. Rev.* **107**, 926 (2007).
- [nelson_modeling_2009](#) [28] J. Nelson, J. J. Kwiakowski, J. Kirkpatrick, and J. M. Frost, *Accounts Chem. Res.* **42**, 1768 (2009). [17](#)
- [marcus_electron_1993](#) [29] R. A. Marcus, *Rev. Mod. Phys.* **65**, 599 (1993). [17](#)

- [hutchison_hopping_2005](#) [30] G. R. Hutchison, M. A. Ratner, and T. J. Marks, *J. Am. Chem. Soc.* **127**, 2339 (2005). [17](#)
- [chang_new_2005](#) [31] J.-L. Chang, *J. Mol. Spectrosc.* **232**, 102 (2005). [18](#)
- [hoffman_reorganization_1996](#) [32] B. M. Hoffman and M. A. Ratner, *Inorg. Chim. Acta.* **243**, 233 (1996). [18](#)
- [bortz_new_1975](#) [33] A. B. Bortz, M. H. Kalos, and J. L. Lebowitz, *J. Comput. Phys.* **17**, 10 (1975). [19](#)
- [scher_anomalous_1975](#) [34] H. Scher and E. Montroll, *Phys. Rev. B* **12**, 2455 (1975). [19](#)
- [borsenberger_role_1993](#) [35] P. M. Borsenberger, E. H. Magin, M. D. VanAuweraer, and F. C. D. Schryver, *Phys. Status Solidi A* **140**, 9 (1993). [19](#)
- [derrida_velocity_1983](#) [36] B. Derrida, *J. Stat. Phys.* **31**, 433 (1983). [19](#), [21](#)
- [cordes_one-dimensional_2001](#) [37] H. Cordes et al., *Phys. Rev. B* **63**, 094201 (2001).
- [seki_electric_2001](#) [38] K. Seki and M. Tachiya, *Phys. Rev. B* **65**, 014305 (2001). [19](#)
- [lukyanov_extracting_2010](#) [39] A. Lukyanov and D. Andrienko, *Phys. Rev. B* **82**, 193202 (2010). [19](#)
- [van_der_holst_modeling_2009](#) [40] J. J. M. van der Holst et al., *Phys. Rev. B* **79**, 085203 (2009). [21](#)
- [dunlap_charge-dipole_1996](#) [41] D. Dunlap, P. Parris, and V. Kenkre, *Phys. Rev. Lett.* **77**, 542 (1996). [21](#)
- [novikov_essential_1998](#) [42] S. V. Novikov et al., *Phys. Rev. Lett.* **81**, 4472 (1998). [21](#)
- [nagata_atomistic_2008](#) [43] Y. Nagata and C. Lennartz, *J. Chem. Phys.* **129**, 034709 (2008). [21](#)
- [novikov_cluster_1995](#) [44] S. V. Novikov and A. V. Vannikov, *J. Phys. Chem.* **99**, 14573 (1995). [21](#)